Robust Transmission Design for RIS-Assisted Secure Multiuser Communication Systems in the Presence of Hardware Impairments

Zhangjie Peng[®], Ruisong Weng, Cunhua Pan[®], Senior Member, IEEE, Gui Zhou[®], Member, IEEE, Marco Di Renzo[®], Fellow, IEEE, and A. Lee Swindlehurst[®], Fellow, IEEE

Abstract—This paper investigates reconfigurable intelligent surface (RIS)-assisted secure multiuser communication systems in the presence of hardware impairments (HIs) at the RIS and the transceivers. We jointly optimize the beamforming vectors at the base station (BS) and the phase shifts of the reflecting elements at the RIS so as to maximize the weighted minimum approximate ergodic secrecy rate (WMAESR), subject to the transmission power constraints at the BS and unit-modulus constraints at the RIS. To solve the formulated optimization problem, we first decouple it into two tractable subproblems and then use the block coordinate descent (BCD) method to alternately optimize the subproblems. Two different methods are proposed to solve the two obtained subproblems. The first method transforms each subproblem into a second order cone programming (SOCP)

Manuscript received 27 April 2022; revised 9 October 2022 and 8 January 2023; accepted 19 February 2023. Date of publication 9 March 2023; date of current version 13 November 2023. The work of Zhangjie Peng was supported in part by the Natural Science Foundation of Shanghai under Grant 22ZR1445600; in part by the National Natural Science Foundation of China under Grant 61701307; and in part by the Open Research Fund of National Mobile Communications Research Laboratory, Southeast University, under Grant 2018D14. The work of Cunhua Pan was supported in part by the National Natural Science Foundation of China under Grant 62201137. The work of Gui Zhou was supported by the Alexander von Humboldt Foundation. The work of Marco Di Renzo was supported in part by the European Commission through the H2020 ARIADNE Project under Agreement 871464 and through the H2020 RISE-6G Project under Agreement 101017011. The work of A. Lee Swindlehurst was supported by the U.S. National Science Foundation under Grant ECCS-2030029 and Grant CNS-2107182. The associate editor coordinating the review of this article and approving it for publication was Y.-F. Liu. (Corresponding authors: Cunhua Pan; Ruisong Weng.)

Zhangjie Peng is with the College of Information, Mechanical and Electrical Engineering, Shanghai Normal University, Shanghai 200234, China, also with the National Mobile Communications Research Laboratory, Southeast University, Nanjing 210096, China, and also with the Shanghai Engineering Research Center of Intelligent Education and Bigdata, Shanghai Normal University, Shanghai 200234, China (e-mail: pengzhangjie@shnu.edu.cn).

Ruisong Weng is with the College of Information, Mechanical and Electrical Engineering, Shanghai Normal University, Shanghai 200234, China (e-mail: 1000497102@smail.shnu.edu.cn).

Cunhua Pan is with the National Mobile Communications Research Laboratory, Southeast University, Nanjing 210096, China (e-mail: cpan@seu.edu.cn). Gui Zhou is with the Institute for Digital Communications, Friedrich-

Gui Zhou is with the Institute for Digital Communications, Friedrich-Alexander-Universität Erlangen-Nürnberg (FAU), 91054 Erlangen, Germany (e-mail: gui.zhou@fau.de).

Marco Di Renzo is with Université Paris-Saclay, CNRS, CentraleSupélec, Laboratoire des Signaux et Systèmes, 91192 Gif-sur-Yvette, France (e-mail: marco.di-renzo@universite-paris-saclay.fr).

A. Lee Swindlehurst is with the Department of Electrical Engineering and Computer Science, University of California Irvine, Irvine, CA 92697 USA (e-mail: swindle@uci.edu).

Color versions of one or more figures in this article are available at https://doi.org/10.1109/TWC.2023.3252046.

Digital Object Identifier 10.1109/TWC.2023.3252046

problem by invoking the penalty convex-concave procedure (CCP) method and the closed-form fractional programming (FP) criterion, and then directly solves them by using CVX. The second method leverages the minorization-maximization (MM) algorithm. Specifically, we first derive a concave approximation function, which is a lower bound of the original objective function, and then the two subproblems are transformed into two simple surrogate problems that admit closed-form solutions. Simulation results verify the performance gains of the proposed robust transmission methods over existing non-robust designs. In addition, the MM algorithm is shown to have much lower complexity than the SOCP-based algorithm.

Index Terms—Intelligent reflecting surface (IRS), reconfigurable intelligent surface (RIS), hardware impairments (HIs), physical layer security (PLS).

I. Introduction

THANKS to the growing popularization of mobile devices, the global wireless network capacity is expected to increase 100-fold by 2030 [1]. Furthermore, emerging applications, such as the industrial Internet of things, virtual reality (VR) and augmented reality (AR) [2], have high quality of service (QoS) requirements, such as ultra-low latency, ultra-high reliability and extremely high data rates [3]. Some promising technologies, such as massive multiple-input multiple-output (m-MIMO) systems, millimeter wave (mmWave) and terahertz (THz) communications [4], have been proposed to meet these demanding requirements. However, these technologies usually result in increasing the cost of network deployment and the network power consumption [5].

Another emerging technology for fulfilling the high QoS requirements of future networks [6], [7] is the use of reconfigurable intelligent surfaces (RISs). RIS is a thin metamaterial layer that is composed of an array of low cost reflecting elements integrated with low power and controllable electronics [8]. Due to the absence of power amplifiers, digital signal processing units, and multiple radio frequency chains, the main features of an RIS include a low implementation cost, a low power consumption, and an easy deployment, as well as the capability of reconfiguring the wireless environment [9], [10]. Broadly speaking, an RIS is a dynamic metasurface whose electromagnetic characteristics can be dynamically adjusted through control signals. For example, the electromagnetic waves that impinge upon an RIS can be steered towards different directions, by simply optimizing the phase response of each of its constituent scattering elements [11]. An RIS can

1536-1276 © 2023 IEEE. Personal use is permitted, but republication/redistribution requires IEEE permission. See https://www.ieee.org/publications/rights/index.html for more information.

be utilized to enhance the desired signal power, to mitigate the network interference, and to reduce the electromagnetic pollution since no additional signals are generated [12]. Compared with traditional active antenna arrays that are equipped with multiple active radio frequency transceivers, an RIS reradiates the incident signals by simply adjusting the amplitude and the phase shift of the reflecting elements, which can be realized by controlling the junction voltage of PIN diodes or varactors [13]. RISs can be deployed on, e.g., the facades of buildings, the interior walls of offices, and windows.

RISs can be utilized for enhancing the security of wireless networks and have been recently amalgamated with physical layer security (PLS) as well [14], [15]. Traditional wireless security methods encrypt the data at the network layer. This usually requires a high overhead due to the frequent distribution and management of secrecy keys [16], [17], [18]. PLS is an alternative solution that makes use of the properties of the wireless communication medium and the transceiver hardware to enable secure communications. However, conventional PLS techniques only focus on beamforming design at the transceivers, and may not provide good performance in some scenarios, e.g., when the legitimate user and the eavesdropper have highly correlated channels (such as when they are located in the same direction with respect to the transmitter) [19]. Thanks to the capability of reconfiguring the propagation environment in a desired manner, an RIS can change the phase of each incident signal so as to enhance the desired signal power at the legitimate users, while suppressing the signal received by the eavesdroppers. RISs have several applications in the context of PLS for improving the security of wireless communication systems [20], [21], [22], [23]. For example, the authors of [20] studied the secrecy outage probability of an RIS-assisted single-antenna system where only one eavesdropper exist. In [21], the authors proposed a robust algorithm to maximize the achievable secrecy rate in a multi-user multiple-input single-output (MISO) system. In [22], the authors proposed a deep reinforcement learning (DRL)-based scheme to improve the security performance of RIS-assisted MIMO systems. The authors of [23] analyzed the security performance gains when deploying an RIS in unmanned aerial vehicle (UAV)-assisted mmWave wireless communication networks.

The existing contributions on RIS-assisted PLS assume that the transceivers are constructed with ideal and perfect hardware components. In practical communication systems, low-cost hardware is often preferred even though such hardware may be subject to hardware impairments (HIs), such as I/Q-imbalances, amplifier non-linearities, quantization errors, and phase noise [24]. If these hardware impairments are ignored at the design stage, the performance usually degrades [25]. Recently, the impact of HIs on the security performance of RIS-assisted single-user systems has been analyzed [26], [27]. Specifically, the authors of [26] proposed a robust algorithm to maximize the secrecy rate in the presence of HIs. In [27], the authors derived an approximated closed-form expression for the secrecy outage probability and studied the impact of HIs on the system performance.

In this paper, we investigate the security performance of RIS-assisted multiuser MISO systems in the presence of HIs. Unlike the single-user scenarios considered in [26]

and [27], we assume a scenario with multiple legitimate users whose information security is threatened by an eavesdropper. By deploying an RIS, we aim to improve the security performance under the premise of ensuring fairness among the users. However, due to the considered complex scenario, the resulting optimization problem cannot be directly solved by using existing methods. Thus, we propose tractable algorithms to tackle the formulated optimization problem. Specifically, the main contributions of this paper are summarized as follows:

- This work is the first to consider RIS-aided secure communications in multiuser MISO systems, where the base station (BS), the RIS and the legitimate users are subject to HIs. By optimizing the BS precoding matrix and the RIS reflection coefficients, we formulate a fairness-based joint optimization problem that maximizes the weighted minimum approximate ergodic secrecy rate (WMAESR), subject to transmit power and unit modulus constraints.
- 2) To efficiently solve the non-convex problem, we propose a benchmark algorithm based on the block coordinate descent (BCD) method. Specifically, we first decouple the original problem into multiple tractable subproblems by invoking the penalty convex-concave procedure (CCP) and the closed-form fractional programming (FP) criterion. The precoding and the reflection coefficient subproblems are transformed into second order cone programming (SOCP) problems. Then, the two obtained subproblems are alternately solved until convergence.
- 3) Also, we propose a minorization-maximization (MM) algorithm to reduce the computational complexity. In particular, we first derive a concave smooth function as a lower bound of the original non-differentiable objective function. Then, we apply the MM algorithm to obtain a surrogate function which has a closed-form solution.
- 4) Finally, we present simulation results to verify the effectiveness of the proposed schemes and the advantages of the proposed robust transmission design for secure communications. We demonstrate that deploying an RIS can effectively improve the security performance of multiuser wireless communication systems in the presence of HIs. The convergence and effectiveness of the proposed algorithm are verified as well.

The rest of this paper is organized as follows. Section II introduces the RIS-assisted wireless communication system model subject to HIs and formulates the WMAESR problem. Section III decouples the original problem into multiple tractable sub-problems and proposes a benchmark optimization algorithm based on the BCD method. In Section IV, a low-complexity MM algorithm is introduced. Simulation results are given in Section V, and Section VI concludes this paper.

Notations: Constants, column vectors and matrices are denoted by italics, boldface lowercase letters and boldface uppercase letters, respectively. Re $\{b\}$, |b| and $\angle(b)$ denote the real part, modulus and angle of the complex number b, respectively. $[b]^+$ denotes $\max(b,0)$. $\|\mathbf{b}\|_1$, $\|\mathbf{b}\|_2$ and $\|\mathbf{b}\|_F$ denote the 1-norm, 2-norm and Frobenius-norm of vector \mathbf{b} , respectively. diag (\cdot) and vec (\cdot) represent the diagonalization and vectorization operators, respectively. \mathbf{B}^{T} , \mathbf{B}^* , \mathbf{B}^{H} , $\mathrm{Tr}\left[\mathbf{B}\right]$

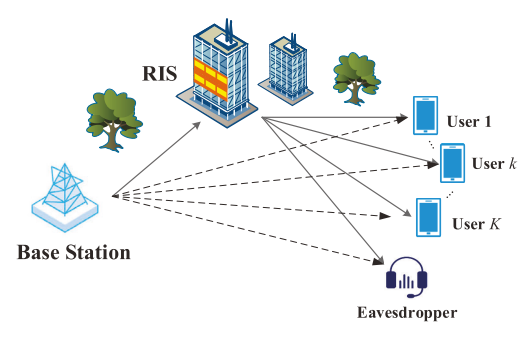


Fig. 1. An RIS-assisted MISO downlink system with an N-antenna BS. a single-antenna eavesdropper and K single-antenna users.

and $\|\mathbf{B}\|_F$ denote the transpose, conjugate, Hermitian, trace and Frobenius norm of matrix B, respectively. The Hadamard product and Kronecker product of two matrices B and C are expressed as $B \odot C$ and $B \otimes C$, respectively. $B \succeq C$ indicates that B - C is a positive semidefinite matrix. I_K denotes the $K \times K$ identity matrix. \mathbb{C} denotes the complex field and $j \triangleq \sqrt{-1}$ is the imaginary unit.

II. SYSTEM MODEL

A. Signal Transmission Model

We consider an RIS-assisted MISO downlink system with a BS, an eavesdropper and K legitimate users, as illustrated in Fig. 1. The BS is equipped with N > 1 transmit antennas to serve the legitimate users in the presence of the eavesdropper. In addition, an RIS consisting of M reflecting elements is deployed to ensure the secure transmission of data. The reflection coefficient of the m-th reflecting element of the RIS is denoted by $\phi_m = e^{j\theta_m}$, where $\theta_m \in [0, 2\pi]$ is the phase shift. The set of RIS reflection coefficients is collected in the diagonal matrix $\mathbf{\Phi} = \operatorname{diag}(\boldsymbol{\phi})$, where $\boldsymbol{\phi} = [\phi_1, \cdots, \phi_M]^{\mathrm{T}}$ with $|\phi_m|^2 = 1, m \in \mathcal{M}, \mathcal{M} \triangleq \{1, 2, \dots, M\}. \mathbf{\Lambda} = \operatorname{diag}(\boldsymbol{\psi})$ is the random phase noise matrix, wherein $\psi = [\psi_1, \dots, \psi_M]^T$ and $\psi_m = e^{j\vartheta_m}$. The phase ϑ_m is the m-th RIS element's phase noise caused by the presence of HIs at the RIS, which is assumed uniformly distributed in $[-\pi/2, \pi/2]$ [28]. The direct channels from the BS to the legitimate user k and from the BS to the eavesdropper, the indirect channel from the BS to the RIS, and the reflection channels from the RIS to the legitimate user k and from the RIS to the eavesdropper, are denoted by $\mathbf{h}_{\mathrm{BU},k} \in \mathbb{C}^{N\times 1}$, $\mathbf{h}_{\mathrm{BE}} \in \mathbb{C}^{N\times 1}$, $\mathbf{H}_{\mathrm{BR}} \in \mathbb{C}^{M\times N}$, $\mathbf{h}_{\mathrm{RU},k} \in \mathbb{C}^{M\times 1}$ and $\mathbf{h}_{\mathrm{RE}} \in \mathbb{C}^{M\times 1}$, respectively.

The signal transmitted by the BS is given by

$$\mathbf{x} = \sum_{k=1}^{K} \mathbf{w}_k s_k + \boldsymbol{\eta}_t \triangleq \hat{\mathbf{x}} + \boldsymbol{\eta}_t, \tag{1}$$

where s_k is assumed to be an independent Gaussian random variable with zero mean and variance $\mathbb{E}\left|\left|s_k\right|^2\right|$ In addition, $\mathbf{w}_k \in \mathbb{C}^{N \times 1}$ is the corresponding beamforming vector. Hence, the precoding matrix of the BS is defined as $\mathbf{W} \triangleq [\mathbf{w}_1, \cdots, \mathbf{w}_K] \in \mathbb{C}^{N \times K}$, which satisfies the constraint $\mathrm{Tr}(\mathbf{W}^{\mathrm{H}}\mathbf{W}) \leqslant P$, where P represents the maximum transmit power. The additional distortion noise term $\eta_{
m t}$ describes the

¹The analysis of reflection models with phase-dependent amplitude [29], [30], [31] is postponed to a future research work.

impact of the HIs at the transmitter. According to the model in [32] and [33], the distortion noise is assumed to be proportional to the signal power. In particular, the entries of η_{+} are independent zero-mean Gaussian random variables whose distribution is $\mathcal{CN}(0, \Upsilon_t)$, where $\Upsilon_t = \kappa_t \mathrm{diag}\left(\mathbf{W}\mathbf{W}^H\right)$ and $\kappa_{\rm t} \geqslant 0$ is the ratio between the transmit distorted noise power and the transmit signal power.

The signal received at user k is given by

$$y_{\mathrm{U},k} = \mathbf{h}_{\mathrm{U},k}^{\mathrm{H}} \mathbf{x} + \eta_{\mathrm{r},k} + n_{\mathrm{U},k} \triangleq \hat{y}_{\mathrm{U},k} + \eta_{\mathrm{r},k}, \qquad (2)$$
 where $\mathbf{h}_{\mathrm{U},k}^{\mathrm{H}} \triangleq \mathbf{h}_{\mathrm{RU},k}^{\mathrm{H}} \mathbf{\Lambda} \mathbf{\Phi} \mathbf{H}_{\mathrm{BR}} + \mathbf{h}_{\mathrm{BU},k}^{\mathrm{H}}$ and $n_{\mathrm{U},k}$ is the additive white Gaussian noise (AWGN) whose distribution is $\mathcal{CN}(0, \delta_{\mathrm{U},k}^2)$. Also, $\eta_{\mathrm{r},k}$ is an additional distortion noise term that is independent of $\hat{y}_{\mathrm{U},k}$ and whose distribution is $\mathcal{CN}(0, \varrho_{\mathrm{r},k})$, with $\varrho_{\mathrm{r},k}$ being defined as $\varrho_{\mathrm{r},k} = \mathbb{E}\left\{\kappa_{\mathrm{r},k} \|\hat{y}_{\mathrm{U},k}\|_2^2\right\}$, where $\kappa_{\mathrm{r},k} \geqslant 0$ is the ratio between the distorted noise power and the undistorted received signal

The achievable rate of user k in nat/second/Hertz (nat/s/Hz) is given by

$$R_{\mathrm{U}\,k} = \log\left(1 + \gamma_{\mathrm{U}\,k}\right),\tag{3}$$

where

power [26].

$$\gamma_{\mathrm{U},k} \triangleq \frac{\mathbf{w}_{k}^{\mathrm{H}} \mathbf{h}_{\mathrm{U},k} \mathbf{h}_{\mathrm{U},k}^{\mathrm{H}} \mathbf{w}_{k}}{\sum_{\substack{i=1\\i\neq k}}^{K} \mathbf{w}_{i}^{\mathrm{H}} \mathbf{h}_{\mathrm{U},k} \mathbf{h}_{\mathrm{U},k}^{\mathrm{H}} \mathbf{w}_{i} + \mathbf{h}_{\mathrm{U},k}^{\mathrm{H}} \boldsymbol{\Upsilon}_{\mathrm{t}} \mathbf{h}_{\mathrm{U},k} + \varrho_{\mathrm{r},k} + \delta_{\mathrm{U},k}^{2}}.$$
(4)

We consider the worst-case assumption that the eavesdropper can eliminate most of the noise with the exception of the distortion noise due to the hardware at the transmitter. Also, we assume that the eavesdropper can decode and cancel the interference from other users [34]. In addition, the eavesdropper is assumed to actively attack the communication system. Specifically, by pretending to be a legitimate user sending pilot signals to the BS during the channel estimation phase [35], the eavesdropper can mislead the BS to send signals to the eavesdropper. Furthermore, low-complexity channel estimation methods [36], [37] can be adopted to estimate the RIS-user and RIS-eavesdropper channels. Then, the signal received at the eavesdropper is given by

$$y_{\rm E} = \mathbf{h}_{\rm E}^{\rm H} \mathbf{x} + n_{\rm E},\tag{5}$$

 $y_{\rm E} = \mathbf{h}_{\rm E}^{\rm H} \mathbf{x} + n_{\rm E}, \tag{5}$ where $\mathbf{h}_{\rm E}^{\rm H} \triangleq \mathbf{h}_{\rm RE}^{\rm H} \boldsymbol{\Lambda} \boldsymbol{\Phi} \mathbf{H}_{\rm BR} + \mathbf{h}_{\rm BE}^{\rm H}$ and $n_{\rm E}$ is the AWGN whose distribution is $\mathcal{CN}(0, \delta_{\rm E}^2)$. Then, the achievable rate of the eavesdropper associated with user k is

$$R_{\mathrm{E},k} = \log \left(1 + \frac{\mathbf{w}_{k}^{\mathrm{H}} \mathbf{h}_{\mathrm{E}} \mathbf{h}_{\mathrm{E}}^{\mathrm{H}} \mathbf{w}_{k}}{\mathbf{h}_{\mathrm{E}}^{\mathrm{H}} \mathbf{\Upsilon}_{\mathrm{t}} \mathbf{h}_{\mathrm{E}} + \delta_{\mathrm{E}}^{2}} \right).$$
 (6)

B. HIs Model

We focus on the ergodic secrecy rate that is defined as $\bar{R}_k =$ $\left[\mathbb{E}\left\{R_{\mathrm{U},k}\right\} - \mathbb{E}\left\{R_{\mathrm{E},k}\right\}\right]^{+}$ and the expectation is taken over the randomness of Λ . However, the expression of the exact \bar{R}_k is difficult to compute, due to the expectation operator outside the logarithmic symbol [38]. Hence, we utilize [39, Lemma 1] to obtain the approximate ergodic secrecy rate (AESR) of user k as follows

$$\bar{R}_k \approx \widehat{R_{\mathrm{U},k}} - \widehat{R_{\mathrm{E},k}},$$
 (7)

where

$$\widehat{R_{\mathrm{U},k}} \triangleq \log\left(1 + \widehat{\gamma_{\mathrm{U},k}}\right),\tag{8}$$

$$\widehat{R_{\mathrm{E},k}} \triangleq \log \left(1 + \frac{\mathbf{w}_{k}^{\mathrm{H}} \mathbb{E} \left\{ \mathbf{h}_{\mathrm{E}} \mathbf{h}_{\mathrm{E}}^{\mathrm{H}} \right\} \mathbf{w}_{k}}{\mathrm{Tr} \left[\mathbf{\Upsilon}_{t} \mathbb{E} \left\{ \mathbf{h}_{\mathrm{E}} \mathbf{h}_{\mathrm{E}}^{\mathrm{H}} \right\} \right] + \delta_{\mathrm{E}}^{2}} \right), \quad (9)$$

based on the definitions given in (10) bottom of the page.

To apply the approximation, we need to calculate $\mathbb{E}_{\psi}\left\{\psi^*\psi^{\mathrm{T}}\right\}$ and $\mathbb{E}_{\psi}\left\{\psi^*\right\}$. To this end, we denote $\delta_{\vartheta}=$ $\vartheta_i - \vartheta_j, i, j \in \mathcal{M}$. Since ϑ_i and ϑ_j are uniformly distributed in $[-\pi/2,\pi/2]$, their probability density function is $f(\vartheta_i) = \frac{1}{\pi}$. Hence, δ_{ϑ} follows a triangular distribution in $[-\pi, \pi]$, whose probability density function is [28]

$$f\left(\delta_{\vartheta}\right) = \begin{cases} \frac{1}{\pi^{2}}\delta_{\vartheta} + \frac{1}{\pi}, & \delta_{\vartheta} \in [-\pi, 0], \\ -\frac{1}{\pi^{2}}\delta_{\vartheta} + \frac{1}{\pi}, & \delta_{\vartheta} \in [0, \pi]. \end{cases}$$
Therefore, we have $\mathbb{E}_{\delta_{\vartheta}}\left\{e^{j\vartheta_{i} - j\vartheta_{j}}\right\} = \mathbb{E}_{\delta_{\vartheta}}\left\{e^{j\delta_{\vartheta}}\right\} =$

 $\int_{-\pi}^{\pi} f(\delta_{\vartheta}) e^{j\delta_{\vartheta}} d\delta_{\vartheta} = \frac{4}{\pi^2}$, and $\mathbb{E}_{\psi} \left\{ \psi^* \psi^{\mathrm{T}} \right\}$ can be formulated as in (14), shown at the bottom of the page, where

$$[\mathbf{G}]_{(i,j)} = \begin{cases} 0, & i = j, \\ \frac{4}{\pi^2}, & i \neq j. \end{cases}$$
 (15)

In addition, we have $\mathbb{E}_{\vartheta_i}\left\{e^{-j\vartheta_i}\right\} = \int_{-\frac{\pi}{2}}^{\frac{\pi}{2}} f\left(\vartheta_i\right) \left(\cos\vartheta_i - j\sin\vartheta_i\right) d\vartheta_i = \frac{2}{\pi}$, and we hence obtain

$$\mathbb{E}_{\boldsymbol{\psi}}\left\{\boldsymbol{\psi}^*\right\} = \frac{2}{\pi}\mathbf{1},\tag{16}$$

where 1 represents the unit column vector with all elements equal to one. By substituting (14) and (16) into (11), we have $\mathbb{E}\left\{\mathbf{h}_{\mathrm{U},k}\mathbf{h}_{\mathrm{H}|k}^{\mathrm{H}}\right\}$

$$= 2\operatorname{Re}\left\{\mathbf{H}_{\mathrm{BR}}^{\mathrm{H}}\mathbf{\Phi}^{\mathrm{H}}\operatorname{diag}\left(\mathbf{h}_{\mathrm{RU},k}\right)\frac{2}{\pi}\mathbf{1}\mathbf{h}_{\mathrm{BU},k}^{\mathrm{H}}\right\} \\ + \mathbf{H}_{\mathrm{BR}}^{\mathrm{H}}\mathbf{\Phi}^{\mathrm{H}}\operatorname{diag}\left(\mathbf{h}_{\mathrm{RU},k}\right)\left(\mathbf{I}_{M} + \mathbf{G}\right)\operatorname{diag}\left(\mathbf{h}_{\mathrm{RU},k}^{\mathrm{H}}\right)\mathbf{\Phi}\mathbf{H}_{\mathrm{BR}} \\ + \mathbf{h}_{\mathrm{BU},k}\mathbf{h}_{\mathrm{BU},k}^{\mathrm{H}}$$

$$= \mathbf{H}_{\mathrm{BR}}^{\mathrm{H}} \mathbf{\Phi}^{\mathrm{H}} \mathrm{diag} \left(\mathbf{h}_{\mathrm{RU},k} \right) \mathbf{T} \mathbf{T}^{\mathrm{T}} \mathrm{diag} \left(\mathbf{h}_{\mathrm{RU},k}^{\mathrm{H}} \right) \mathbf{\Phi} \mathbf{H}_{\mathrm{BR}} \\ + \left(\frac{2}{\pi} \mathbf{H}_{\mathrm{BR}}^{\mathrm{H}} \mathbf{\Phi}^{\mathrm{H}} \mathbf{h}_{\mathrm{RU},k} + \mathbf{h}_{\mathrm{BU},k} \right) \left(\frac{2}{\pi} \mathbf{h}_{\mathrm{RU},k}^{\mathrm{H}} \mathbf{\Phi} \mathbf{H}_{\mathrm{BR}} + \mathbf{h}_{\mathrm{BU},k}^{\mathrm{H}} \right)$$

$$= \hat{\mathbf{h}}_{\mathrm{U},k} \hat{\mathbf{h}}_{\mathrm{U},k}^{\mathrm{H}} + \hat{\mathbf{H}}_{\mathrm{U},k} \hat{\mathbf{H}}_{\mathrm{U},k}^{\mathrm{H}} = \bar{\mathbf{H}}_{\mathrm{U},k} \bar{\mathbf{H}}_{\mathrm{U},k}^{\mathrm{H}},$$
(17)

where $\bar{\mathbf{H}}_{\mathrm{U},k} \triangleq [\hat{\mathbf{h}}_{\mathrm{U},k} \ \hat{\mathbf{H}}_{\mathrm{U},k}], \hat{\mathbf{h}}_{\mathrm{U},k}^{\mathrm{H}} \triangleq \frac{2}{\pi} \mathbf{h}_{\mathrm{RU},k}^{\mathrm{H}} \mathbf{\Phi} \mathbf{H}_{\mathrm{BR}} + \mathbf{h}_{\mathrm{BU},k}^{\mathrm{H}}$ (8) $\hat{\mathbf{H}}_{\mathrm{U},k}^{\mathrm{H}} \triangleq \mathbf{T}^{\mathrm{T}} \mathrm{diag} \left(\mathbf{h}_{\mathrm{RU},k}^{\mathrm{H}} \right) \mathbf{\Phi} \mathbf{H}_{\mathrm{BR}} \text{ and } \mathbf{T} \mathbf{T}^{\mathrm{T}}$ (9) diag $\left(\left(1-\frac{4}{\pi^2}\right)\mathbf{I}_M\right)$.

By definition, $arrho_{\mathrm{r},k}=\mathbb{E}\left\{\kappa_{\mathrm{r},k}\left\|\hat{y}_{\mathrm{U},k}\right\|_{2}^{2}\right\}$. Hence, $arrho_{\mathrm{r},k}$ can be

$$\varrho_{r,k} = \text{Tr}\left[\kappa_{r,k} \left(\mathbf{W}\mathbf{W}^{H} + \kappa_{t} \text{diag}\left(\mathbf{W}\mathbf{W}^{H}\right)\right) \bar{\mathbf{H}}_{U,k} \bar{\mathbf{H}}_{U,k}^{H}\right] + \kappa_{r,k} \delta_{U,k}^{2},$$
(18)

and $\widehat{R_{\mathrm{U},k}}$ is given by

$$\widehat{R_{\mathrm{U},k}} = \log\left(1 + \widehat{\gamma_{\mathrm{U},k}}\right),\tag{19}$$

where

$$\widehat{\gamma_{\mathbf{U},k}} \triangleq \frac{\left\|\bar{\mathbf{H}}_{\mathbf{U},k}^{\mathbf{H}} \mathbf{w}_{k}\right\|_{2}^{2}}{\sum_{\substack{i=1\\i\neq k}}^{K} \left\|\bar{\mathbf{H}}_{\mathbf{U},k}^{\mathbf{H}} \mathbf{w}_{i}\right\|_{2}^{2} + \operatorname{Tr}\left[\Upsilon_{t} \bar{\mathbf{H}}_{\mathbf{U},k} \bar{\mathbf{H}}_{\mathbf{U},k}^{\mathbf{H}}\right] + \varrho_{\mathbf{r},k} + \delta_{\mathbf{U},k}^{2}}.$$
(20)

Similarly, by substituting (14) and (16) into (12), we have

$$\widehat{R_{\mathrm{E},k}} = \log\left(1 + \frac{\left\|\bar{\mathbf{H}}_{\mathrm{E}}^{\mathrm{H}}\mathbf{w}_{k}\right\|_{2}^{2}}{\operatorname{Tr}\left[\mathbf{\Upsilon}_{\mathrm{t}}\bar{\mathbf{H}}_{\mathrm{E}}\bar{\mathbf{H}}_{\mathrm{E}}^{\mathrm{H}}\right] + \delta_{\mathrm{E}}^{2}}\right),\tag{21}$$

where $\mathbb{E}_{\psi}\left\{\mathbf{h}_{\mathrm{E}}\mathbf{h}_{\mathrm{E}}^{\mathrm{H}}\right\} = \bar{\mathbf{H}}_{\mathrm{E}}\bar{\mathbf{H}}_{\mathrm{E}}^{\mathrm{H}}, \; \bar{\mathbf{H}}_{\mathrm{E}} \triangleq [\hat{\mathbf{h}}_{\mathrm{E}}\;\hat{\mathbf{H}}_{\mathrm{E}}], \; \hat{\mathbf{H}}_{\mathrm{E}}^{\mathrm{H}} \triangleq$ $\mathbf{T}^{\mathrm{T}}\mathrm{diag}\left(\mathbf{h}_{\mathrm{RE}}^{\mathrm{H}}\right)\mathbf{\Phi}\mathbf{H}_{\mathrm{BR}} \text{ and } \mathbf{\hat{h}}_{\mathrm{E}}^{\mathrm{H}}\triangleq \tfrac{2}{\pi}\mathbf{h}_{\mathrm{RE}}^{\mathrm{H}}\mathbf{\Phi}\mathbf{H}_{\mathrm{BR}}+\mathbf{h}_{\mathrm{BE}}^{\mathrm{H}}.$

Accordingly, the AESR $\widehat{R_k}$ of the legitimate user k is given by [38]

$$\widehat{R}_{k} \triangleq \left[\widehat{R_{\mathrm{U},k}} - \widehat{R_{\mathrm{E},k}} \right]^{+}. \tag{22}$$

C. Problem Formulation

To maximize the WMAESR while ensuring fairness, we consider the weighted joint optimization of the precoding matrix W and the reflection coefficient vector ϕ . By denoting the weighting factor of user k by ω_k , the WMAESR maximization problem is formulated as

$$\max_{\mathbf{W}, \phi} \min_{k \in \mathcal{K}} \left\{ \omega_k \widehat{R}_k \right\}
\text{s.t. } \mathbf{W} \in \mathcal{S}_{\mathbf{W}},$$
(23a)

s.t.
$$\mathbf{W} \in \mathcal{S}_{\mathbf{W}}$$
, (23b)

$$\phi \in \mathcal{S}_{\phi},$$
 (23c)

$$\widehat{\gamma_{\mathrm{U},k}} \triangleq \frac{\mathbf{w}_{k}^{\mathrm{H}} \mathbb{E} \left\{ \mathbf{h}_{\mathrm{U},k} \mathbf{h}_{\mathrm{U},k}^{\mathrm{H}} \right\} \mathbf{w}_{k}}{\sum\limits_{\substack{i=1\\i\neq k}}^{K} \mathbf{w}_{i}^{\mathrm{H}} \mathbb{E} \left\{ \mathbf{h}_{\mathrm{U},k} \mathbf{h}_{\mathrm{U},k}^{\mathrm{H}} \right\} \mathbf{w}_{i} + \mathrm{Tr} \left[\mathbf{\Upsilon}_{\mathrm{t}} \mathbb{E} \left\{ \mathbf{h}_{\mathrm{U},k} \mathbf{h}_{\mathrm{U},k}^{\mathrm{H}} \right\} \right] + \varrho_{\mathrm{r},k} + \delta_{\mathrm{U},k}^{2}}.$$
(10)

$$\mathbb{E}\left\{\mathbf{h}_{\mathrm{U},k}\mathbf{h}_{\mathrm{U},k}^{\mathrm{H}}\right\} = 2\mathrm{Re}\left\{\mathbf{H}_{\mathrm{BR}}^{\mathrm{H}}\mathbf{\Phi}^{\mathrm{H}}\mathrm{diag}\left(\mathbf{h}_{\mathrm{RU},k}\right)\mathbb{E}_{\psi}\left\{\psi^{*}\right\}\mathbf{h}_{\mathrm{BU},k}^{\mathrm{H}}\right\} + \mathbf{h}_{\mathrm{BU},k}\mathbf{h}_{\mathrm{BU},k}^{\mathrm{H}}$$
$$+\mathbf{H}_{\mathrm{BR}}^{\mathrm{H}}\mathbf{\Phi}^{\mathrm{H}}\mathrm{diag}\left(\mathbf{h}_{\mathrm{RU},k}\right)\mathbb{E}_{\psi}\left\{\psi^{*}\psi^{\mathrm{T}}\right\}\mathrm{diag}\left(\mathbf{h}_{\mathrm{RU},k}^{\mathrm{H}}\right)\mathbf{\Phi}\mathbf{H}_{\mathrm{BR}}.$$
(11)

$$\mathbb{E}\left\{\mathbf{h}_{\mathrm{E}}\mathbf{h}_{\mathrm{E}}^{\mathrm{H}}\right\} = 2\operatorname{Re}\left\{\mathbf{H}_{\mathrm{BR}}^{\mathrm{H}}\mathbf{\Phi}^{\mathrm{H}}\operatorname{diag}\left(\mathbf{h}_{\mathrm{RE}}\right)\mathbb{E}_{\boldsymbol{\psi}}\left\{\boldsymbol{\psi}^{*}\right\}\mathbf{h}_{\mathrm{BE}}^{\mathrm{H}}\right\} + \mathbf{h}_{\mathrm{BE}}\mathbf{h}_{\mathrm{BE}}^{\mathrm{H}}$$
$$+\mathbf{H}_{\mathrm{BR}}^{\mathrm{H}}\mathbf{\Phi}^{\mathrm{H}}\operatorname{diag}\left(\mathbf{h}_{\mathrm{RE}}\right)\mathbb{E}_{\boldsymbol{\psi}}\left\{\boldsymbol{\psi}^{*}\boldsymbol{\psi}^{\mathrm{T}}\right\}\operatorname{diag}\left(\mathbf{h}_{\mathrm{RE}}^{\mathrm{H}}\right)\mathbf{\Phi}\mathbf{H}_{\mathrm{BR}}.\tag{12}$$

$$\mathbb{E}_{\boldsymbol{\psi}} \left\{ \boldsymbol{\psi}^* \boldsymbol{\psi}^{\mathrm{T}} \right\} = \mathbf{I}_M + \mathbf{G} = \begin{pmatrix}
1 & \mathbb{E}_{\delta_{\vartheta}} \left\{ e^{j\vartheta_1 - j\vartheta_2} \right\} & \cdots & \mathbb{E}_{\delta_{\vartheta}} \left\{ e^{j\vartheta_M - j\vartheta_1} \right\} \\
\mathbb{E}_{\delta_{\vartheta}} \left\{ e^{j\vartheta_1 - j\vartheta_2} \right\} & 1 & \cdots & \mathbb{E}_{\delta_{\vartheta}} \left\{ e^{j\vartheta_M - j\vartheta_2} \right\} \\
\vdots & \vdots & \ddots & \vdots \\
\mathbb{E}_{\delta_{\vartheta}} \left\{ e^{j\vartheta_1 - j\vartheta_M} \right\} & \mathbb{E}_{\delta_{\vartheta}} \left\{ e^{j\vartheta_2 - j\vartheta_M} \right\} & \cdots & 1
\end{pmatrix}, \tag{14}$$

where $S_{W} \triangleq \{\mathbf{W} | \mathrm{Tr}(\mathbf{W}^{H}\mathbf{W}) \leq P\}, \ \mathcal{K} \triangleq \{1, 2, \dots, K\},$ $\mathcal{M} \triangleq \{1, 2, \dots, M\}$ and the set $\mathcal{S}_{\phi} \triangleq \{\phi | |\phi_m| = 1, m \in \mathcal{M}\}$ accounts for the unit-modulus constraint on ϕ . Compared to the corresponding system model with no HIs, the objective function of the problem in (23) is more complex. The analysis of the AESR instead of the information rate further complicates the objective function to the point that a direct solution becomes intractable. To circumvent these issues, we propose two efficient algorithms in the next sections.

III. BCD-SOCP ALGORITHM

In this section, we propose a BCD-SOCP algorithm to solve the problem in (23). Specifically, we first decouple the problem in (23) into two subproblems, each of which is converted into an SOCP problem that can be efficiently solved. The two subproblems are then alternately solved until convergence.

A. Problem Reformulation

To reduce the complexity of the objective function in (23), we write $\widehat{R_k}$ as the sum of three parts, i.e.,

$$\widehat{R}_{k}(\mathbf{W}, \boldsymbol{\phi}) = \widehat{R}_{\mathbf{U},k}(\mathbf{W}, \boldsymbol{\phi}) - \widehat{R}_{\mathbf{E},k}(\mathbf{W}, \boldsymbol{\phi})
= \widehat{R}_{\mathbf{U},k}(\mathbf{W}, \boldsymbol{\phi}) - \log \left(\frac{\|\bar{\mathbf{H}}_{\mathbf{E}}^{\mathbf{H}} \mathbf{w}_{k}\|_{2}^{2} + \operatorname{Tr} \left[\boldsymbol{\Upsilon}_{\mathbf{t}} \bar{\mathbf{H}}_{\mathbf{E}} \bar{\mathbf{H}}_{\mathbf{E}}^{\mathbf{H}} \right] + \delta_{\mathbf{E}}^{2}}{\operatorname{Tr} \left[\boldsymbol{\Upsilon}_{\mathbf{t}} \bar{\mathbf{H}}_{\mathbf{E}} \bar{\mathbf{H}}_{\mathbf{E}}^{\mathbf{H}} \right] + \delta_{\mathbf{E}}^{2}} \right)
= f_{1,k}(\mathbf{W}, \boldsymbol{\phi}) + f_{2,k}(\mathbf{W}, \boldsymbol{\phi}) + f_{3}(\mathbf{W}, \boldsymbol{\phi}), \tag{24}$$

where

$$f_{1,k}(\mathbf{W}, \boldsymbol{\phi}) \triangleq \widehat{R_{\mathbf{U},k}}(\mathbf{W}, \boldsymbol{\phi}), \qquad (25)$$

$$(\mathbf{H}\mathbf{\bar{H}}^{\mathbf{H}}\mathbf{w}, \|^{2} + \operatorname{Tr}\left[\boldsymbol{\Upsilon}, \mathbf{\bar{H}}_{\mathbf{D}}\mathbf{\bar{H}}^{\mathbf{H}}\right] \setminus$$

$$f_{2,k}(\mathbf{W}, \boldsymbol{\phi}) \triangleq -\log \left(1 + \frac{\left\| \bar{\mathbf{H}}_{E}^{H} \mathbf{w}_{k} \right\|_{2}^{2} + \operatorname{Tr} \left[\boldsymbol{\Upsilon}_{t} \bar{\mathbf{H}}_{E} \bar{\mathbf{H}}_{E}^{H} \right]}{\delta_{E}^{2}} \right),$$
(26)

$$f_3(\mathbf{W}, \boldsymbol{\phi}) \triangleq \log \left(1 + \frac{\text{Tr} \left[\boldsymbol{\Upsilon}_t \bar{\mathbf{H}}_E \bar{\mathbf{H}}_E^H \right]}{\delta_E^2} \right).$$
 (27)

In the following, we derive lower bounds for $f_{1,k}$, $f_{2,k}$ and f_3 , respectively.

As far as $f_{1,k}$ is concerned, we derive a lower bound by applying the closed-form FP approach [40]. First of all, $f_{1,k}$ can be tackled based on the following lemma.

Lemma 1: Consider the function $f(\bar{y}) = \log(1 + \bar{y}) - \bar{y} + \bar{y}$ $\frac{(1+\bar{y})\bar{x}}{1+\bar{x}}$ for any $\bar{x}>0$. Then, we have

$$\log\left(1+\bar{x}\right) = \max_{\bar{y} \geqslant 0} \ f\left(\bar{y}\right),\tag{28}$$

and the optimal solution is $\bar{y} = \bar{x}$.

The lemma provides a lower bound for $\log (1 + \bar{x})$, which is tight when $\bar{y} = \bar{x}$. Hence, by introducing a set of auxiliary variables $\mathcal{V} = \{v_k \ge 0, k \in \mathcal{K}\}$, we have

$$f_{1,k}(\mathbf{W}, \boldsymbol{\phi}, \mathcal{V}) \geqslant \log(1 + v_k) - v_k + \frac{(1 + v_k)\widehat{\gamma_{\mathbf{U},k}}}{1 + \widehat{\gamma_{\mathbf{U},k}}}.$$
 (29)

The variables $\mathbf{W}, \phi, \mathcal{V}$ are coupled together due to the term $\frac{1+v_k)\hat{\gamma_{U,k}}}{1+\hat{\gamma_{U,k}}}$. To tackle this coupling, we introduce a set of auxiliary variables $\mathcal{U} = \{\mathbf{u}_k \in \mathbb{C}^{(M+1)\times 1}, k \in \mathcal{K}\}$ and adopt the quadratic transform [40]. Therefore, a lower bound for $f_{1,k}$ can be expressed as

$$\tilde{f}_{1,k}(\mathbf{W}, \boldsymbol{\phi}, \mathcal{U}, \mathcal{V}) = \log(1 + v_k) + 2\sqrt{(1 + v_k)} \operatorname{Re} \left\{ \mathbf{u}_k^{\mathrm{H}} \bar{\mathbf{H}}_{\mathrm{U},k}^{\mathrm{H}} \mathbf{w}_k \right\}
- v_k - (1 + \kappa_{\mathrm{r},k}) \delta_{\mathrm{U},k}^2 \mathbf{u}_k^{\mathrm{H}} \mathbf{u}_k - (1 + \kappa_{\mathrm{r},k}) \mathbf{u}_k^{\mathrm{H}} \mathbf{u}_k
\times \operatorname{Tr} \left[\left(\mathbf{W} \mathbf{W}^{\mathrm{H}} + \kappa_{\mathrm{t}} \operatorname{diag} \left(\mathbf{W} \mathbf{W}^{\mathrm{H}} \right) \right) \bar{\mathbf{H}}_{\mathrm{U},k} \bar{\mathbf{H}}_{\mathrm{U},k}^{\mathrm{H}} \right]. (30)$$

The relation between $f_{1,k}$ and $\tilde{f}_{1,k}$ is

$$f_{1,k}(\mathbf{W}, \phi) = \max_{\mathcal{U}, \mathcal{V}} \tilde{f}_{1,k}(\mathbf{W}, \phi, \mathcal{U}, \mathcal{V}), \tag{31}$$

where the optimal $\mathbf{u}_k^{\text{opt}}$ and v_k^{opt} are given in (32) and (33), shown at the bottom of the page, respectively.

As far as $f_{2,k}$ is concerned, we introduce the following lemma to obtain a lower bound.

Lemma 2 [41]: Consider the function $f(\bar{y}) = -\bar{y}\bar{x} + \log \bar{y} +$ 1 for any $\bar{x} > 0$. Then, we have

$$-\log \bar{x} = \max_{\bar{y} > 0} f(\bar{y}), \qquad (34)$$

and the optimal solution is $\bar{y} = \frac{1}{\bar{z}}$.

The lemma shows that $f(\bar{y})$ is a lower bound of $-\log \bar{x}$, and the bound is tight when $\bar{y} = \frac{1}{\bar{x}}$. Let us denote $\mathcal{D} =$ $\{d_k\geqslant 0, k\in\mathcal{K}\}$ and define $\bar{x}=1+\frac{\left\|\bar{\mathbf{H}}_{\mathrm{E}}^{\mathrm{H}}\mathbf{w}_k\right\|_2^2+\mathrm{Tr}\left[\mathbf{\Upsilon}_{\mathrm{t}}\bar{\mathbf{H}}_{\mathrm{E}}\bar{\mathbf{H}}_{\mathrm{E}}^{\mathrm{H}}\right]}{\delta_{\mathrm{E}}^2}$ $\bar{y}=d_k.$ Then, a lower bound for $f_{2,k}$ is given by $\tilde{f}_{2,k}$, which is defined as

$$f_{2,k}(\mathbf{W}, \boldsymbol{\phi}) = \max_{\mathcal{D}} \ \tilde{f}_{2,k}(\mathbf{W}, \boldsymbol{\phi}, \mathcal{D}),$$
 (35)

$$\tilde{f}_{2,k}(\mathbf{W}, \boldsymbol{\phi}, \mathcal{D}) = -d_k \left(1 + \frac{\|\bar{\mathbf{H}}_{\mathrm{E}}^{\mathrm{H}} \mathbf{w}_k\|_2^2 + \mathrm{Tr}[\mathbf{\Upsilon}_{\mathrm{t}} \bar{\mathbf{H}}_{\mathrm{E}} \bar{\mathbf{H}}_{\mathrm{E}}^{\mathrm{H}}]}{\delta_{\mathrm{E}}^2} \right) + \log d_k + 1, \tag{36}$$

and the optimal solution for d_k is

$$d_k^{\text{opt}} = \left(1 + \frac{\left\|\bar{\mathbf{H}}_{\text{E}}^{\text{H}} \mathbf{w}_k\right\|_2^2 + \text{Tr}\left[\boldsymbol{\Upsilon}_{\text{t}} \bar{\mathbf{H}}_{\text{E}} \bar{\mathbf{H}}_{\text{E}}^{\text{H}}\right]}{\delta_{\text{E}}^2}\right)^{-1}.$$
 (37)

Finally, to find a lower bound for f_3 that is given in a tractable analytical form, we utilize the following lemma.

Lemma 3 [42]: Given the complex vector $\bar{\mathbf{y}}$, the function $f(\bar{\mathbf{y}}, \bar{\mathbf{x}}) = \left(\|\bar{\mathbf{x}}\|_{2}^{2} + \delta^{2}\right) \|\bar{\mathbf{y}}\|_{2}^{2} - 2\operatorname{Re}\left\{\bar{\mathbf{y}}^{H}\bar{\mathbf{x}}\right\} + 1 \text{ satisfies}$ $\frac{\delta^{2}}{\|\bar{\mathbf{x}}\|_{2}^{2} + \delta^{2}} = \min_{\bar{\mathbf{y}}} f(\bar{\mathbf{y}}, \bar{\mathbf{x}}),$

$$\frac{\delta^2}{\|\bar{\mathbf{x}}\|_2^2 + \delta^2} = \min_{\bar{\mathbf{y}}} f(\bar{\mathbf{y}}, \bar{\mathbf{x}}), \qquad (38)$$

and the optimal solution is $\bar{\mathbf{y}} = \frac{\bar{\mathbf{x}}}{\|\bar{\mathbf{x}}\|_2^2 + \delta^2}$.

The lemma provides an upper bound for $\frac{\delta^2}{\|\bar{\mathbf{x}}\|_2^2 + \delta^2}$, which is tight when $\bar{\mathbf{y}} = \frac{\bar{\mathbf{x}}}{\|\bar{\mathbf{x}}\|_2^2 + \delta^2}$. Then, let us introduce a new variable $\tilde{\mathbf{w}} = \text{vec}(\tilde{\mathbf{W}}), \tilde{\mathbf{w}} \in \mathcal{S}_{\tilde{\mathbf{w}}} \triangleq \{\tilde{\mathbf{w}} | \tilde{\mathbf{w}}^{H} \tilde{\mathbf{w}} \leq P\}$. Due to the complexity of f_3 , we derive the corresponding lower bounds for the following two cases: 1) Case A: Given the other variables, $\tilde{\mathbf{w}}$ is the only variable to be optimized; 2) Case B: Given the other variables, ϕ is the only variable to be optimized.

$$\mathbf{u}_{k}^{\text{opt}} = \frac{\sqrt{(1+v_{k})}\bar{\mathbf{H}}_{\mathrm{U},k}^{\mathrm{H}}\mathbf{w}_{k}}{(1+\kappa_{\mathrm{r},k})\left(\operatorname{Tr}\left[\left(\mathbf{W}\mathbf{W}^{\mathrm{H}}+\kappa_{\mathrm{t}}\operatorname{diag}\left(\mathbf{W}\mathbf{W}^{\mathrm{H}}\right)\right)\bar{\mathbf{H}}_{\mathrm{U},k}\bar{\mathbf{H}}_{\mathrm{U},k}^{\mathrm{H}}\right]+\delta_{\mathrm{U},k}^{2}\right)},$$
(32)

$$v_{\nu}^{\text{opt}} = \widehat{\gamma_{\text{U}k}}$$
 (33)

1) Case A: Given the other variables, $\tilde{\mathbf{w}}$ is the only variable to be optimized. Based on Lemma 2 and Lemma 3, a lower bound for $f_3(\tilde{\mathbf{w}})$ is obtained as stated in the following

Lemma 4: Let us introduce the auxiliary variables $p_{\rm w}$ and \mathbf{q}_{w} . A lower bound for $f_3(\tilde{\mathbf{w}})$ is given by

$$\tilde{f}_{3,\tilde{\mathbf{w}}}(\tilde{\mathbf{w}}) = -\tilde{\mathbf{w}}^{\mathrm{H}}\tilde{\mathbf{C}}_{3,\mathrm{w}}\tilde{\mathbf{w}} + 2\mathrm{Re}\left\{\tilde{\mathbf{b}}_{3,\mathrm{w}}^{\mathrm{H}}\tilde{\mathbf{w}}\right\} + \tilde{c}_{3,\mathrm{w}},$$
 (39)

where
$$\tilde{\mathbf{C}}_{3,w} \triangleq p_w \|\mathbf{q}_w\|_2^2 \mathbf{L} \mathbf{L}^T$$
, $\tilde{\mathbf{b}}_{3,w} \triangleq p_w \mathbf{L} \mathbf{q}_w$, $\tilde{c}_{3,w} \triangleq -p_w \|\mathbf{q}_w\|_2^2 \delta_{\mathrm{E}}^2 - p_w + \log p_w + 1$, $\mathbf{L} \mathbf{L}^T \triangleq \kappa_t \left(\mathbf{I}_K \otimes \operatorname{diag}\left(\bar{\mathbf{H}}_{\mathrm{E}} \bar{\mathbf{H}}_{\mathrm{E}}^H\right)\right)$.

Additionally, the optimal solutions for p_w and q_w are given by

$$p_{\rm w}^{\rm opt} = \left(1 + \frac{\text{Tr}\left[\mathbf{\Upsilon}_{\rm t}\bar{\mathbf{H}}_{\rm E}\bar{\mathbf{H}}_{\rm E}^{\rm H}\right]}{\delta_{\rm E}^2}\right),\tag{40}$$

$$\mathbf{q}_{\mathbf{w}}^{\mathbf{opt}} = \frac{\mathbf{L}^{\mathrm{T}} \tilde{\mathbf{w}}}{\|\mathbf{L}^{\mathrm{T}} \tilde{\mathbf{w}}\|_{2}^{2} + \delta_{\mathrm{E}}^{2}}.$$
 (41)

Proof: See [43, Appendix A].

2) Case B: Given the other variables, ϕ is the only variable to be optimized. Based on Lemma 1 and Lemma 2, a lower bound for $f_3(\phi)$ is obtained as stated in the following lemma.

Lemma 5: Let us introduce the auxiliary variables p_{ϕ} and \mathbf{Q}_{ϕ} , and denote $\hat{\mathbf{q}}_{\phi}$ and $\hat{\mathbf{Q}}_{\phi}$ as $\mathbf{Q}_{\phi} = [\hat{\mathbf{q}}_{\phi} \ \hat{\mathbf{Q}}_{\phi}]$. A lower bound for $f_3(\phi)$ is given by

$$\tilde{f}_{3,\phi}\left(\phi\right) = -\phi^{\mathrm{H}}\tilde{\mathbf{C}}_{3,\phi}\phi + 2\mathrm{Re}\left\{\tilde{\mathbf{b}}_{3,\phi}^{\mathrm{H}}\phi\right\} + \tilde{c}_{3,\phi},$$
 (42)

where $\tilde{c}_{3,\phi} \triangleq -p_{\phi} + \log p_{\phi} + 1 - p_{\phi} \|\mathbf{Q}_{\phi}\|_{F}^{2} \mathbf{h}_{\mathrm{BE}}^{\mathrm{H}} \mathbf{J} \mathbf{J}^{\mathrm{T}} \mathbf{h}_{\mathrm{BE}} - p_{\phi} \|\mathbf{Q}_{\phi}\|_{F}^{2} \delta_{\mathrm{E}}^{2} + 2p_{\phi} \mathrm{Re} \left\{ \mathrm{Tr} \left[\mathbf{J} \hat{\mathbf{q}}_{\phi} \mathbf{h}_{\mathrm{BE}}^{\mathrm{H}} \right] \right\}, \mathbf{J} \mathbf{J}^{\mathrm{T}} \triangleq \Upsilon_{\mathrm{t}}, \ \tilde{\mathbf{C}}_{3,\phi} \triangleq p_{\phi} \|\mathbf{Q}_{\phi}\|_{F}^{2} \mathbf{C}_{3,\phi}, \ \tilde{\mathbf{b}}_{3,\phi} \triangleq p_{\phi} \mathbf{a}_{3,\phi}^{*} - p_{\phi} \|\mathbf{Q}_{\phi}\|_{F}^{2} \mathbf{b}_{3,\phi} \ \text{and}$

$$\mathbf{C}_{3,\phi} \triangleq \left(\left(\frac{4}{\pi^2} \mathbf{h}_{\mathrm{RE}} \mathbf{h}_{\mathrm{RE}}^{\mathrm{H}} \right) \odot \left(\mathbf{H}_{\mathrm{BR}} \mathbf{J} \mathbf{J}^{\mathrm{T}} \mathbf{H}_{\mathrm{BR}}^{\mathrm{H}} \right)^{\mathrm{T}} \right) \\ + \left(\left(\operatorname{diag} \left(\mathbf{h}_{\mathrm{RE}} \right) \mathbf{T} \mathbf{T}^{\mathrm{T}} \operatorname{diag} \left(\mathbf{h}_{\mathrm{RE}}^{\mathrm{H}} \right) \right) \\ \odot \left(\mathbf{H}_{\mathrm{BR}} \mathbf{J} \mathbf{J}^{\mathrm{T}} \mathbf{H}_{\mathrm{BR}}^{\mathrm{H}} \right)^{\mathrm{T}} \right),$$

$$\mathbf{b}_{3,\phi}^{\mathrm{H}} \triangleq \mathbf{h}_{\mathrm{RE}}^{\mathrm{H}} \mathrm{diag} \left(\mathbf{H}_{\mathrm{BR}} \mathbf{J} \mathbf{J}^{\mathrm{T}} \mathbf{h}_{\mathrm{BE}} \right),$$

$$\mathbf{a}_{3,\phi} \triangleq \left[\left[\frac{2}{\pi} \mathbf{H}_{\mathrm{BR}} \mathbf{J} \hat{\mathbf{q}}_{\phi} \mathbf{h}_{\mathrm{RE}}^{\mathrm{H}} + \mathbf{H}_{\mathrm{BR}} \mathbf{J} \hat{\mathbf{Q}}_{\phi} \mathbf{T}^{\mathrm{T}} \operatorname{diag} \left(\mathbf{h}_{\mathrm{RE}}^{\mathrm{H}} \right) \right]_{1,1}, \dots, \right.$$
$$\left[\frac{2}{\pi} \mathbf{H}_{\mathrm{BR}} \mathbf{J} \hat{\mathbf{q}}_{\phi} \mathbf{h}_{\mathrm{RE}}^{\mathrm{H}} + \mathbf{H}_{\mathrm{BR}} \mathbf{J} \hat{\mathbf{Q}}_{\phi} \mathbf{T}^{\mathrm{T}} \operatorname{diag} \left(\mathbf{h}_{\mathrm{RE}}^{\mathrm{H}} \right) \right]_{M,M}^{\mathrm{T}}.$$

Additionally, the optimal solutions for p_{ϕ} and \mathbf{Q}_{ϕ} are given

$$p_{\phi}^{\text{opt}} = \left(1 + \frac{\text{Tr}\left[\mathbf{\Upsilon}_{\text{t}}\bar{\mathbf{H}}_{\text{E}}\bar{\mathbf{H}}_{\text{E}}^{\text{H}}\right]}{\delta_{\text{E}}^{2}}\right),\tag{43}$$

$$\mathbf{Q}_{\phi}^{\text{opt}} = \frac{\mathbf{J}^{\text{T}} \bar{\mathbf{H}}_{\text{E}}}{\left\| \mathbf{J}^{\text{T}} \bar{\mathbf{H}}_{\text{E}} \right\|_{F}^{2} + \delta_{\text{E}}^{2}}$$
(44)

Proof: See [43, Appendix B].

Thus, by denoting $\mathcal{P} = \{p_{\mathbf{w}}, p_{\phi}\}, \ \mathcal{Q} = \{\mathbf{q}_{\mathbf{w}}, \mathbf{Q}_{\phi}\}, \ \text{a lower}$ bound for f_3 is expressed as

$$\tilde{f}_{3}(\tilde{\mathbf{w}}, \boldsymbol{\phi}, \mathcal{P}, \mathcal{Q}) \triangleq \begin{cases} \tilde{f}_{3,\tilde{\mathbf{w}}}(\tilde{\mathbf{w}}, \boldsymbol{\phi}, \mathcal{P}, \mathcal{Q}), & \text{Case A} \\ \tilde{f}_{3,\boldsymbol{\phi}}(\tilde{\mathbf{w}}, \boldsymbol{\phi}, \mathcal{P}, \mathcal{Q}), & \text{Case B} \end{cases} . (45)$$

Finally, from (24), (30), (35) and (45), a lower bound for R_k can be formulated as

$$\tilde{R}_{k} = \left[\tilde{f}_{1,k}(\tilde{\mathbf{w}}, \boldsymbol{\phi}, \mathcal{U}, \mathcal{V}) + \tilde{f}_{2,k}(\tilde{\mathbf{w}}, \boldsymbol{\phi}, \mathcal{D}) + \tilde{f}_{3}(\tilde{\mathbf{w}}, \boldsymbol{\phi}, \mathcal{P}, \mathcal{Q})\right]^{+}.$$
(46)

Eventually, the problem in (23) can be reformulated as

$$\max_{\tilde{\mathbf{w}}, \boldsymbol{\phi}, \mathcal{U}, \mathcal{V}, \mathcal{D}, \mathcal{P}, \mathcal{Q}} \min_{k \in \mathcal{K}} \left\{ \omega_k \tilde{R}_k \right\}$$
 (47a)

s.t.
$$\tilde{\mathbf{w}} \in \mathcal{S}_{\tilde{\mathbf{w}}}$$
, (47b)

$$\phi \in \mathcal{S}_{\phi}.$$
 (47c)

To solve the problem in (47), we use the BCD method to alternately optimize each variable in the objective function, while keeping the other variables fixed. The optimal solutions for \mathcal{U} , \mathcal{V} , \mathcal{D} , \mathcal{P} and \mathcal{Q} are given in (32), (33), (37), (40), (43), (41), and (44), respectively. On the other hand, the optimization of the precoding vector $\tilde{\mathbf{w}}$ and the reflection coefficient vector ϕ are addressed in the following sections.

B. Optimization of the Precoding Vector $\tilde{\mathbf{w}}$

In this subsection, $\tilde{\mathbf{w}}$ is optimized under the assumption that all the other variables are kept fixed. Since the lower bound $f_{3,\tilde{\mathbf{w}}}$ in (39) is a quadratic function in the optimization variable, we rewrite $f_{1,k}\left(\tilde{\mathbf{w}}\right)$ and $f_{2,k}\left(\tilde{\mathbf{w}}\right)$ as quadratic functions as well.

1) Mathematical Derivation of $f_{1,k}(\tilde{\mathbf{w}})$. Let us denote by \mathbf{t}_k the vector whose single non-zero element is one at the k-th position. Then, $f_{1,k}(\tilde{\mathbf{w}})$ in (30) can be reformulated as

$$\begin{split} \tilde{f}_{1,k}\left(\tilde{\mathbf{w}}\right) &= 2\sqrt{(1+v_k)}\mathrm{Re}\left\{\mathrm{Tr}\left[\mathbf{t}_k\mathbf{u}_k^H\bar{\mathbf{H}}_{\mathrm{U},k}^H\mathbf{W}\right]\right\} \\ &+ \tilde{c}_{1,\mathrm{w},k} - (1+\kappa_{\mathrm{r},k})\,\mathbf{u}_k^H\mathbf{u}_k \\ &\times \mathrm{Tr}\left[\mathbf{W}^H\left(\bar{\mathbf{H}}_{\mathrm{U},k}\bar{\mathbf{H}}_{\mathrm{U},k}^H+\kappa_{\mathrm{t}}\mathrm{diag}\left(\bar{\mathbf{H}}_{\mathrm{U},k}\bar{\mathbf{H}}_{\mathrm{U},k}^H\right)\right)\mathbf{W}\right] \\ &= 2\mathrm{Re}\left\{\mathrm{Tr}\left[\mathbf{B}_{1,\mathrm{w},k}\mathbf{W}\right]\right\} - \mathrm{Tr}\left[\mathbf{W}^H\mathbf{C}_{1,\mathrm{w},k}\mathbf{W}\right] + \tilde{c}_{1,\mathrm{w},k}, \ (48) \\ \text{where} \quad \mathbf{B}_{1,\mathrm{w},k} &\triangleq \sqrt{(1+v_k)}\mathbf{t}_k\mathbf{u}_k^H\bar{\mathbf{H}}_{\mathrm{U},k}^H, \quad \tilde{c}_{1,\mathrm{w},k} &\triangleq \\ \log\left(1+v_k\right) - v_k - \left(1+\kappa_{\mathrm{r},k}\right)\delta_{\mathrm{U},k}^2\mathbf{u}_k^H\mathbf{u}_k \ \text{and} \ \mathbf{C}_{1,\mathrm{w},k} &\triangleq \\ \left(1+\kappa_{\mathrm{r},k}\right)\mathbf{u}_k^H\mathbf{u}_k(\bar{\mathbf{H}}_{\mathrm{U},k}\bar{\mathbf{H}}_{\mathrm{U},k}^H) + \quad \kappa_{\mathrm{t}}\mathrm{diag}(\bar{\mathbf{H}}_{\mathrm{U},k}\bar{\mathbf{H}}_{\mathrm{U},k}^H)). \\ \mathrm{Then}, \quad \mathrm{by} \quad \mathrm{using} \quad \mathrm{the} \quad \mathrm{identity} \quad \mathrm{Tr}\left[\mathbf{A}\mathbf{B}\mathbf{C}\right] &= \\ \left(\mathrm{vec}\left(\mathbf{A}^\mathrm{T}\right)\right)^\mathrm{T}\left(\mathbf{I}\otimes\mathbf{B}\right)\mathrm{vec}\left(\mathbf{C}\right) \quad \mathrm{and} \quad \mathrm{Tr}\left[\mathbf{A}^\mathrm{T}\mathbf{D}\right] &= \\ \left(\mathrm{vec}\left(\mathbf{A}\right)\right)^\mathrm{T}\mathrm{vec}\left(\mathbf{D}\right)\left[44\right], \ \mathrm{we} \ \mathrm{have} \end{split}$$

$$\operatorname{vec}(\mathbf{A}) \operatorname{vec}(\mathbf{C}) \quad \text{and} \quad \operatorname{II}[\mathbf{A} \ \mathbf{B}] = \operatorname{vec}(\mathbf{A})^{\operatorname{T}} \operatorname{vec}(\mathbf{D}) \quad [44], \text{ we have}$$

$$\tilde{f}_{1,k}(\tilde{\mathbf{w}}) = 2\operatorname{Re}\left\{\tilde{\mathbf{b}}_{1,\mathrm{w},k}^{\operatorname{H}}\tilde{\mathbf{w}}\right\} - \tilde{\mathbf{w}}^{\operatorname{H}}\tilde{\mathbf{C}}_{1,\mathrm{w},k}\tilde{\mathbf{w}} + \tilde{c}_{1,\mathrm{w},k},$$

where
$$\tilde{\mathbf{b}}_{1,\mathrm{w},k} \triangleq \mathrm{vec}\left(\mathbf{B}_{1,\mathrm{w},k}^{\mathrm{H}}\right)$$
 and $\tilde{\mathbf{C}}_{1,\mathrm{w},k} \triangleq \mathbf{I}_{K} \otimes \mathbf{C}_{1,\mathrm{w},k}$.

2) Mathematical Derivation of $\tilde{f}_{2,k}(\tilde{\mathbf{w}})$. By using the identity $\operatorname{Tr}[\mathbf{ABCD}] = \left(\operatorname{vec}(\mathbf{D}^{\mathrm{T}})\right)^{\mathrm{T}} \left(\mathbf{C}^{\mathrm{T}} \otimes \mathbf{A}\right) \operatorname{vec}(\mathbf{B})$ [44], $\tilde{f}_{2,k}\left(\tilde{\mathbf{w}}\right)$ in (36) can be reformulated as

$$\tilde{f}_{2,k}\left(\tilde{\mathbf{w}}\right) = -\frac{d_{k}}{\delta_{\mathrm{E},k}^{2}} \left(\operatorname{Tr}\left[\bar{\mathbf{H}}_{\mathrm{E}} \bar{\mathbf{H}}_{\mathrm{E}}^{\mathrm{H}} \mathbf{W} \mathbf{t}_{k} \mathbf{t}_{k}^{\mathrm{H}} \mathbf{W}^{\mathrm{H}} \right] \right. \\
\left. + \kappa_{\mathrm{t}} \operatorname{Tr}\left[\mathbf{W}^{\mathrm{H}} \operatorname{diag}\left(\bar{\mathbf{H}}_{\mathrm{E}} \bar{\mathbf{H}}_{\mathrm{E}}^{\mathrm{H}} \right) \mathbf{W} \right] \right) \\
+ \log d_{k} + 1 - d_{k} \\
= -\frac{d_{k}}{\delta_{\mathrm{E},k}^{2}} \left(\tilde{\mathbf{w}}^{\mathrm{H}} \left(\left(\mathbf{t}_{k} \mathbf{t}_{k}^{\mathrm{H}} \right)^{\mathrm{T}} \otimes \left(\bar{\mathbf{H}}_{\mathrm{E}} \bar{\mathbf{H}}_{\mathrm{E}}^{\mathrm{H}} \right) \right) \tilde{\mathbf{w}} \right. \\
\left. + \kappa_{\mathrm{t}} \tilde{\mathbf{w}}^{\mathrm{H}} \left(\mathbf{I}_{K} \otimes \operatorname{diag} \left(\bar{\mathbf{H}}_{\mathrm{E}} \bar{\mathbf{H}}_{\mathrm{E}}^{\mathrm{H}} \right) \right) \tilde{\mathbf{w}} \right) \\
+ \log d_{k} + 1 - d_{k} \\
= -\tilde{\mathbf{w}}^{\mathrm{H}} \tilde{\mathbf{C}}_{2, \mathbf{w}, k} \tilde{\mathbf{w}} + \tilde{c}_{2, \mathbf{w}, k}, \tag{50}$$

where $\tilde{\mathbf{C}}_{2,\mathrm{w},k} \triangleq \frac{d_k}{\delta_z^2}((\mathbf{t}_k\mathbf{t}_k^{\mathrm{H}})^{\mathrm{T}} \otimes (\bar{\mathbf{H}}_{\mathrm{E}}\bar{\mathbf{H}}_{\mathrm{E}}^{\mathrm{H}})) + \kappa_{\mathrm{t}}(\mathbf{I}_K \otimes$ $\operatorname{diag}(\bar{\mathbf{H}}_{\mathrm{E}}\bar{\mathbf{H}}_{\mathrm{E}}^{\mathrm{H}}))$ and $\tilde{c}_{2,\mathrm{w},k}\!\triangleq\!\log d_{k}+1-d_{k}.$

Substituting (39), (49) and (50) into (47), the subproblem for $\tilde{\mathbf{w}}$ can be transformed into the following equivalent problem

$$\max_{\tilde{\mathbf{w}}} \min_{k \in \mathcal{K}} \left\{ \tilde{r}_{\mathbf{w}, k} \left(\tilde{\mathbf{w}} \right) \right\}
\text{s.t. } \tilde{\mathbf{w}} \in \mathcal{S}_{\tilde{\mathbf{w}}},$$
(51a)

s.t.
$$\tilde{\mathbf{w}} \in \mathcal{S}_{\tilde{\mathbf{w}}}$$
, (51b)

where

$$\tilde{r}_{w,k}(\tilde{\mathbf{w}}) = -\tilde{\mathbf{w}}^{\mathrm{H}}\tilde{\mathbf{C}}_{w,k}\tilde{\mathbf{w}} + 2\mathrm{Re}\left\{\tilde{\mathbf{b}}_{w,k}^{\mathrm{H}}\tilde{\mathbf{w}}\right\} + \tilde{c}_{w,k},$$
 (52)

and $\tilde{\mathbf{C}}_{\mathrm{w},k},\, \tilde{\mathbf{b}}_{\mathrm{w},k}$ and $\tilde{c}_{\mathrm{w},k}$ are defined, respectively, as follows

$$\tilde{\mathbf{C}}_{\mathrm{w},k} \triangleq \omega_k \left(\tilde{\mathbf{C}}_{1,\mathrm{w},k} + \tilde{\mathbf{C}}_{2,\mathrm{w},k} + \tilde{\mathbf{C}}_{3,\mathrm{w}} \right),$$
 (53a)

$$\tilde{\mathbf{b}}_{\mathrm{w},k} \triangleq \omega_k \left(\tilde{\mathbf{b}}_{1,\mathrm{w},k} + \tilde{\mathbf{b}}_{3,\mathrm{w}} \right),$$
 (53b)

$$\tilde{c}_{\mathbf{w},k} \triangleq \omega_k \left(\tilde{c}_{1,\mathbf{w},k} + \tilde{c}_{2,\mathbf{w},k} + \tilde{c}_{3,\mathbf{w}} \right).$$
 (53c)

Finally, by introducing the auxiliary variable $\delta_{\rm w}$, the optimization problem in (51) can be reformulated

$$\max_{\tilde{\omega}} \delta_{\mathbf{w}} \tag{54a}$$

s.t.
$$\tilde{r}_{w,k}(\tilde{\mathbf{w}}) \geqslant \delta_w, k \in \mathcal{K},$$
 (54b)

$$\tilde{\mathbf{w}} \in \mathcal{S}_{\tilde{\mathbf{w}}}.$$
 (54c)

The obtained reformulation in (54) is an SOCP problem whose globally optimum solution $\tilde{\mathbf{w}}$ can be by using standard numerical optimization methods, such as CVX.

C. Optimization of the Reflection Coefficient Vector ϕ

In this subsection, ϕ is optimized under the assumption that all the other variables are kept fixed. The lower bound $f_{3,\phi}$ in (42) is a quadratic function in the optimization variable. Therefore, we rewrite $\tilde{f}_{1,k}(\phi)$ and $\tilde{f}_{2,k}(\phi)$ as quadratic functions.

1) Mathematical Derivation of $\tilde{f}_{1,k}(\phi)$. First of all, $\mathbf{u}_{k}^{\mathrm{H}} \mathbf{\bar{H}}_{\mathrm{II} k}^{\mathrm{H}} \mathbf{w}_{k}$ can be rewritten as

$$\mathbf{u}_{k}^{H}\mathbf{\bar{H}}_{\mathrm{U},k}^{H}\mathbf{w}_{k} = \begin{bmatrix} u_{\phi,k}^{*} & \mathbf{u}_{\phi,k}^{H} \end{bmatrix} \begin{bmatrix} \hat{\mathbf{h}}_{\mathrm{U},k}^{H} \\ \hat{\mathbf{h}}_{\mathrm{U},k}^{H} \end{bmatrix} \mathbf{w}_{k}$$

$$= u_{\phi,k}^{*} \frac{2}{\pi} \mathbf{h}_{\mathrm{RU},k}^{H} \mathbf{\Phi} \mathbf{H}_{\mathrm{BR}} \mathbf{w}_{k} + u_{\phi,k}^{*} \mathbf{h}_{\mathrm{BU},k}^{H} \mathbf{w}_{k}$$

$$+ \mathbf{u}_{\phi,k}^{H} \mathbf{T}^{T} \operatorname{diag} \left(\mathbf{h}_{\mathrm{RU},k}^{H} \right) \mathbf{\Phi} \mathbf{H}_{\mathrm{BR}} \mathbf{w}_{k}$$

$$= \left(\mathbf{u}_{\phi,k}^{H} \mathbf{T}^{T} \operatorname{diag} \left(\mathbf{h}_{\mathrm{RU},k}^{H} \right) \operatorname{diag} \left(\mathbf{H}_{\mathrm{BR}} \mathbf{w}_{k} \right) \right)$$

$$+ u_{\phi,k}^{*} \frac{2}{\pi} \mathbf{h}_{\mathrm{RU},k}^{H} \operatorname{diag} \left(\mathbf{H}_{\mathrm{BR}} \mathbf{w}_{k} \right) \right) \boldsymbol{\phi}$$

$$+ u_{\phi,k}^{*} \mathbf{h}_{\mathrm{BU},k}^{H} \mathbf{w}_{k}$$

$$= \mathbf{a}_{1,\phi,k}^{H} \boldsymbol{\phi} + u_{\phi,k}^{*} \mathbf{h}_{\mathrm{BU},k}^{H} \mathbf{w}_{k}, \qquad (5.1)$$

where $\mathbf{a}_{1,\phi,k}^{\mathrm{H}} \triangleq \mathbf{u}_{\phi,k}^{\mathrm{H}} \mathbf{T}^{\mathrm{T}} \mathrm{diag} \left(\mathbf{h}_{\mathrm{RU},k}^{\mathrm{H}} \right) \mathrm{diag} \left(\mathbf{H}_{\mathrm{BR}} \mathbf{w}_{k} \right) +$ $u_{\phi k}^* \frac{2}{\pi} \mathbf{h}_{\mathrm{BH} k}^{\mathrm{H}} \mathrm{diag} (\mathbf{H}_{\mathrm{BR}} \mathbf{w}_k).$

Denoting $\mathbf{A}_{1,\phi,k} \triangleq (1 + \kappa_{\mathrm{r},k}) \mathbf{u}_k^{\mathrm{H}} \mathbf{u}_k$ $\left(\mathbf{W}\mathbf{W}^{\mathrm{H}} + \kappa_{\mathrm{t}} \mathrm{diag}\left(\mathbf{W}\mathbf{W}^{\mathrm{H}}\right)\right)$ and using the matrix identity

in [44, Eq. (1.10.6)], we have
$$\operatorname{Tr}\left[\bar{\mathbf{H}}_{\mathrm{U},k}^{\mathrm{H}}\mathbf{A}_{1,\phi,k}\bar{\mathbf{H}}_{\mathrm{U},k}\right]$$

$$=\operatorname{Tr}\left[\mathbf{A}_{1,\phi,k}\hat{\mathbf{h}}_{\mathrm{U},k}\hat{\mathbf{h}}_{\mathrm{U},k}^{\mathrm{H}}+\mathbf{A}_{1,\phi,k}\hat{\mathbf{H}}_{\mathrm{U},k}\hat{\mathbf{H}}_{\mathrm{U},k}^{\mathrm{H}}\right]$$

$$=\frac{4}{\pi^{2}}\operatorname{Tr}\left[\boldsymbol{\Phi}^{\mathrm{H}}\mathbf{h}_{\mathrm{RU},k}\mathbf{h}_{\mathrm{RU},k}^{\mathrm{H}}\boldsymbol{\Phi}\mathbf{H}_{\mathrm{BR}}\mathbf{A}_{1,\phi,k}\mathbf{H}_{\mathrm{BR}}^{\mathrm{H}}\right]$$

$$+\operatorname{Tr}\left[\boldsymbol{\Phi}^{\mathrm{H}}\mathrm{diag}\left(\mathbf{h}_{\mathrm{RU},k}\right)\mathbf{T}\mathbf{T}^{\mathrm{T}}\mathrm{diag}\left(\mathbf{h}_{\mathrm{RU},k}^{\mathrm{H}}\right)\right]$$

$$\boldsymbol{\Phi}\mathbf{H}_{\mathrm{BR}}\mathbf{A}_{1,\phi,k}\mathbf{H}_{\mathrm{BR}}^{\mathrm{H}}\right]$$

$$+2\operatorname{Re}\left\{\frac{2}{\pi}\mathbf{h}_{\mathrm{RU},k}^{\mathrm{H}}\boldsymbol{\Phi}\mathbf{H}_{\mathrm{BR}}\mathbf{A}_{1,\phi,k}\mathbf{h}_{\mathrm{BU},k}\right\}$$

$$+\mathbf{h}_{\mathrm{BU},k}^{\mathrm{H}}\mathbf{A}_{1,\phi,k}\mathbf{h}_{\mathrm{BU},k}$$

$$=\boldsymbol{\phi}^{\mathrm{H}}\tilde{\mathbf{C}}_{1,\phi,k}\boldsymbol{\phi}+2\operatorname{Re}\left\{\mathbf{b}_{1,\phi,k}^{\mathrm{H}}\boldsymbol{\phi}\right\}+\mathbf{h}_{\mathrm{BU},k}^{\mathrm{H}}\mathbf{A}_{1,\phi,k}\mathbf{h}_{\mathrm{BU},k},$$
(56)

$$\tilde{\mathbf{C}}_{1,\phi,k} \triangleq \left(\frac{4}{\pi^2} \mathbf{h}_{\mathrm{RU},k} \mathbf{h}_{\mathrm{RU},k}^{\mathrm{H}}\right) \odot \left(\mathbf{H}_{\mathrm{BR}} \mathbf{A}_{1,\phi,k} \mathbf{H}_{\mathrm{BR}}^{\mathrm{H}}\right)^{\mathrm{T}} \\
+ \left(\operatorname{diag}\left(\mathbf{h}_{\mathrm{RU},k}\right) \mathbf{T} \mathbf{T}^{\mathrm{T}} \operatorname{diag}\left(\mathbf{h}_{\mathrm{RU},k}^{\mathrm{H}}\right)\right) \\
\odot \left(\mathbf{H}_{\mathrm{BR}} \mathbf{A}_{1,\phi,k} \mathbf{H}_{\mathrm{BR}}^{\mathrm{H}}\right)^{\mathrm{T}},$$

 $\mathbf{b}_{1,\phi,k}^{\mathrm{H}} \triangleq \frac{2}{\pi} \mathbf{h}_{\mathrm{RU},k}^{\mathrm{H}} \mathrm{diag}\left(\mathbf{H}_{\mathrm{BR}} \mathbf{A}_{1,\phi,k} \mathbf{h}_{\mathrm{BU},k}\right).$ Then, $\tilde{f}_{1,k}(\phi)$ in (30) can be reformulated as

 $f_{1.k}\left(\boldsymbol{\phi}\right)$ $= 2\sqrt{(1+v_k)}\operatorname{Re}\left\{\mathbf{u}_h^{\mathrm{H}}\mathbf{\bar{H}}_{\mathrm{H}h}^{\mathrm{H}}\mathbf{w}_k\right\} + \log\left(1+v_k\right) - v_k$ $-\operatorname{Tr}\left[\bar{\mathbf{H}}_{\mathrm{II},k}^{\mathrm{H}}\mathbf{A}_{1,\phi,k}\bar{\mathbf{H}}_{\mathrm{II},k}\right]-\left(1+\kappa_{\mathrm{r},k}\right)\delta_{\mathrm{II},k}^{2}\mathbf{u}_{k}^{\mathrm{H}}\mathbf{u}_{k}$ $= 2\operatorname{Re}\left\{\tilde{\mathbf{b}}_{1,\phi,k}^{\mathrm{H}}\boldsymbol{\phi}\right\} - \boldsymbol{\phi}^{\mathrm{H}}\tilde{\mathbf{C}}_{1,\phi,k}\boldsymbol{\phi} + \tilde{c}_{1,\phi,k},$ (57)

$$\begin{split} \tilde{\mathbf{b}}_{1,\phi,k} &\triangleq \sqrt{(1+v_k)} \mathbf{a}_{1,\phi,k} - \mathbf{b}_{1,\phi,k}, \\ \tilde{c}_{1,\phi,k} &\triangleq \log\left(1+v_k\right) - v_k - (1+\kappa_{\mathrm{r},k}) \, \delta_{\mathrm{U},k}^2 \mathbf{u}_k^{\mathrm{H}} \mathbf{u}_k \\ &- \mathbf{h}_{\mathrm{BU},k}^{\mathrm{H}} \mathbf{A}_{1,\phi,k} \mathbf{h}_{\mathrm{BU},k} \\ &+ 2\sqrt{(1+v_k)} \mathrm{Re} \left\{ u_{\phi,k}^* \mathbf{h}_{\mathrm{BU},k}^{\mathrm{H}} \mathbf{w}_k \right\}. \end{split}$$

2) Mathematical Derivation of $\tilde{f}_{2,k}\left(\phi\right)$. Similarly, denoting $\mathbf{A}_{2,\phi,k} \triangleq \mathbf{w}_k \mathbf{w}_k^{\mathrm{H}} + \kappa_{\mathrm{t}} \mathrm{diag}(\mathbf{W} \mathbf{W}^{\mathrm{H}}), \ \mathrm{Tr}\left[\bar{\mathbf{H}}_{\mathrm{E}}^{\mathrm{H}} \mathbf{A}_{2,\phi,k} \bar{\mathbf{H}}_{\mathrm{E}}\right] \ \mathrm{can}$ be rewritten as

$$Tr \left[\mathbf{\bar{H}}_{E}^{H} \mathbf{A}_{2,\phi,k} \mathbf{\bar{H}}_{E} \right]$$

$$= Tr \left[\mathbf{A}_{2,\phi,k} \mathbf{\hat{h}}_{E} \mathbf{\hat{h}}_{E}^{H} + \mathbf{A}_{2,\phi,k} \mathbf{\hat{H}}_{E} \mathbf{\hat{H}}_{E}^{H} \right]$$

$$= \frac{4}{\pi^{2}} Tr \left[\mathbf{\Phi}^{H} \mathbf{h}_{RE} \mathbf{h}_{RE}^{H} \mathbf{\Phi} \mathbf{H}_{BR} \mathbf{A}_{2,\phi,k} \mathbf{H}_{BR}^{H} \right]$$

$$+ Tr \left[\mathbf{\Phi}^{H} \operatorname{diag} \left(\mathbf{h}_{RE} \right) \mathbf{T} \mathbf{T}^{T} \operatorname{diag} \left(\mathbf{h}_{RE}^{H} \right) \mathbf{\Phi} \mathbf{H}_{BR} \mathbf{A}_{2,\phi,k} \mathbf{H}_{BR}^{H} \right]$$

$$+ 2 \operatorname{Re} \left\{ \frac{2}{\pi} \mathbf{h}_{RE}^{H} \mathbf{\Phi} \mathbf{H}_{BR} \mathbf{A}_{2,\phi,k} \mathbf{h}_{BE} \right\} + \mathbf{h}_{BE}^{H} \mathbf{A}_{2,\phi,k} \mathbf{h}_{BE}$$

$$= \boldsymbol{\phi}^{H} \mathbf{C}_{2,\phi,k} \boldsymbol{\phi} + 2 \operatorname{Re} \left\{ \mathbf{b}_{2,\phi,k}^{H} \boldsymbol{\phi} \right\} + \mathbf{h}_{BE}^{H} \mathbf{A}_{2,\phi,k} \mathbf{h}_{BE}, \qquad (58)$$
where
$$\mathbf{C}_{2,\phi,k} \triangleq \left(\frac{4}{\pi^{2}} \mathbf{h}_{RE} \mathbf{h}_{RE}^{H} \right) \odot \left(\mathbf{H}_{BR} \mathbf{A}_{2,\phi,k} \mathbf{H}_{BR}^{H} \right)^{T}$$

$$+ \left(\operatorname{diag}(\mathbf{h}_{RE}) \mathbf{T} \mathbf{T}^{T} \operatorname{diag}(\mathbf{h}_{RE}^{H}) \right)$$

$$\odot \left(\mathbf{H}_{BR} \mathbf{A}_{2,\phi,k} \mathbf{H}_{BR}^{H} \right)^{T},$$

$$\mathbf{b}_{2,\phi,k}^{H} \triangleq \frac{2}{\pi} \mathbf{h}_{RE}^{H} \operatorname{diag} \left(\mathbf{H}_{BR} \mathbf{A}_{2,\phi,k} \mathbf{h}_{BE} \right).$$

Then, $f_{2k}(\phi)$ in (36) can be reformulated as

$$\tilde{f}_{2,k}(\boldsymbol{\phi}) = -\frac{d_k}{\delta_{\rm E}^2} \left(\text{Tr} \left[\bar{\mathbf{H}}_{\rm E}^{\rm H} \mathbf{A}_{2,\phi,k} \bar{\mathbf{H}}_{\rm E} \right] \right) + \log d_k + 1 - d_k$$

$$= -\boldsymbol{\phi}^{\rm H} \tilde{\mathbf{C}}_{2,\phi,k} \boldsymbol{\phi} - 2 \text{Re} \left\{ \tilde{\mathbf{b}}_{2,\phi,k}^{\rm H} \boldsymbol{\phi} \right\} + \tilde{c}_{2,\phi,k}, \quad (59)$$

where $\tilde{\mathbf{C}}_{2,\phi,k} \triangleq \frac{d_k}{\delta_{\mathbb{R}}^2} \mathbf{C}_{2,\phi,k}$, $\tilde{\mathbf{b}}_{2,\phi,k} \triangleq \frac{d_k}{\delta_{\mathbb{R}}^2} \mathbf{b}_{2,\phi,k}$ and $\tilde{c}_{2,\phi,k} \triangleq$ $\log d_k + 1 - d_k - \frac{d_k}{\delta_2^2} \mathbf{h}_{\mathrm{BE}}^{\mathrm{H}} \mathbf{A}_{2,\phi,k} \mathbf{h}_{\mathrm{BE}}.$

By substituting (42), (57) and (59) into (47), the optimization subproblem for ϕ is equivalent to

$$\max_{\boldsymbol{\phi}} \min_{k \in \mathcal{K}} \left\{ \tilde{r}_{\boldsymbol{\phi}, k} \left(\boldsymbol{\phi} \right) \right\}$$
s.t. $\boldsymbol{\phi} \in \mathcal{S}_{\boldsymbol{\phi}}$, (60b)

s.t.
$$\phi \in \mathcal{S}_{\phi}$$
, (60b)

where

$$\tilde{r}_{\phi,k}\left(\phi\right) = -\phi^{\mathrm{H}}\tilde{\mathbf{C}}_{\phi,k}\phi + 2\mathrm{Re}\left\{\tilde{\mathbf{b}}_{\phi,k}^{\mathrm{H}}\phi\right\} + \tilde{c}_{\phi,k},$$
 (61)

and $\tilde{\mathbf{C}}_{\phi,k}$, $\tilde{\mathbf{b}}_{\phi,k}$ and $\tilde{c}_{\phi,k}$ are, respectively, given by

$$\tilde{\mathbf{C}}_{\phi,k} \triangleq \omega_k (\tilde{\mathbf{C}}_{1,\phi,k} + \tilde{\mathbf{C}}_{2,\phi,k} + \tilde{\mathbf{C}}_{3,\phi}),$$
 (62a)

$$\tilde{\mathbf{b}}_{\phi,k} \triangleq \omega_k (\tilde{\mathbf{b}}_{1,\phi,k} - \tilde{\mathbf{b}}_{2,\phi,k} + \tilde{\mathbf{b}}_{3,\phi}),$$
 (62b)

$$\tilde{c}_{\phi,k} \triangleq \omega_k \left(\tilde{c}_{1,\phi,k} + \tilde{c}_{2,\phi,k} + \tilde{c}_{3,\phi} \right). \tag{62c}$$

By introducing the auxiliary variable δ_{ϕ} , the problem in (60) can be rewritten as

$$\max_{\Delta} \delta_{\phi} \tag{63a}$$

s.t.
$$\tilde{r}_{\phi,k}(\phi) \geqslant \delta_{\phi}, k \in \mathcal{K},$$
 (63b)

$$\phi \in \mathcal{S}_{\phi}$$
. (63c)

Due to the non-convex unit-modulus constraints in (63c), the problem in (63) is still non-convex. Furthermore, if the semidefinite relaxation (SDR) is used to relax the problem with rank-1 constraint, it would be difficult to obtain a good solution for a phase-only beamforming problem by using Gaussian randomization [45]. Hence, the penalty CCP [46] is used to tackle this issue. To this end, we first note that the constraint (63c) can be equivalently rewritten as $1 \leq$ $|\phi_m|^2 \leqslant 1, m \in \mathcal{M}$. Also, the non-convex parts can be linearized by $\left|\phi_m^{[t]}\right|^2 - 2\text{Re}\left(\phi_m^*\phi_m^{[t]}\right) \leqslant -1$ for any fixed $\phi_m^{[t]}$ at the t-th iteration. By introducing a set of slack variables $\mathbf{b} = [b_1, \dots, b_{2M}]^{\mathrm{T}}$ and a penalty multiplier λ , the problem in (63) can be reformulated as

$$\max_{\boldsymbol{\phi}, \delta_{\phi}, \mathbf{b}} \delta_{\phi} - \lambda \sum_{m=1}^{2M} b_m \tag{64a}$$

s.t.
$$\tilde{r}_{\phi,k}\left(\phi\right) \geqslant \delta_{\phi}, k \in \mathcal{K},$$
 (64b)

$$\left|\phi_m^{[t]}\right|^2 - 2\operatorname{Re}\left(\phi_m^*\phi_m^{[t]}\right) \leqslant b_m - 1, m \in \mathcal{M}, k \in \mathcal{K},$$
(64c)

$$\left|\phi_m\right|^2 \leqslant 1 + b_{M+m},\tag{64d}$$

$$\mathbf{b} \geqslant 0. \tag{64e}$$

The problem in (64) is an SOCP optimization problem, which can be solved by using conventional numerical optimization tools, such as CVX. The details of the proposed penalty CCP algorithm for solving the problem in (64) are summarized in Algorithm 1. More specifically, $\|\phi^{[t]} - \phi^{[t-1]}\|_1 \le$ ε_1 controls the convergence of Algorithm 1, and $\|\mathbf{b}\|_1 \le$ ε_2 guarantees the unit-modulus constraints in (63c), provided that ε_2 is sufficiently small. Additionally, the maximum value $\lambda_{\rm max}$ is introduced to avoid the numerical issues caused by a large λ .

Algorithm 1 Penalty CCP-Based Optimization for RIS Reflection Phase Shifts

```
Initialize: Initialize \overline{\phi^{[0]}} = \phi^{(n)}, \gamma > 1, and set t = 0
  1: while \left\| \boldsymbol{\phi}^{[t]} - \boldsymbol{\phi}^{[t-1]} \right\|_1 > \varepsilon_1 \text{ or } \left\| \mathbf{b} \right\|_1 > \varepsilon_2 \text{ do}
2: Update \boldsymbol{\phi}^{[t+1]} from Problem (64);
3: \lambda^{[t+1]} = \min \left\{ \gamma \lambda^{[t]}, \lambda_{\max} \right\};
   5: end while
```

Algorithm 2 BCD-SOCP Algorithm

6: Output $\phi^{(n+1)} = \phi^{[t]}$

Initialize: Initialize $\tilde{\mathbf{w}}^{(0)}$, $\phi^{(0)}$ to feasible values and set n=0

- 1: while The value of the objective fuction in (47) has not converged
- Given $\tilde{\mathbf{w}}^{(n)}$ and $\phi^{(n)}$, calculate $\mathcal{U}^{(n+1)}$, $\mathcal{V}^{(n+1)}$, $\mathcal{D}^{(n+1)}$, $\mathcal{P}^{(n+1)}$ and $\mathcal{Q}^{(n+1)}$ by using (32), (33), (37), (40), (43), (41)
- Calculate $\tilde{\mathbf{w}}^{(n+1)}$ as the solution of the problem in (54) while $\phi^{(n)}$, $\mathcal{U}^{(n+1)}$, $\mathcal{V}^{(n+1)}$, $\mathcal{D}^{(n+1)}$, $\mathcal{P}^{(n+1)}$ and $\mathcal{Q}^{(n+1)}$ are kept
- Calculate $\phi^{(n+1)}$ via Algorithm 1 while $\tilde{\mathbf{w}}^{(n+1)}$, $\mathcal{U}^{(n+1)}$, $\mathcal{V}^{(n+1)}$, $\mathcal{D}^{(n+1)}$, $\mathcal{P}^{(n+1)}$ and $\mathcal{Q}^{(n+1)}$ are kept fixed;
- Set $n \leftarrow n+1$
- 6: end while

D. Algorithm Development

- 1) BCD-SOCP Algorithm: In Algorithm 2, we present the complete BCD-SOCP algorithm. Specifically, we maximize the WMAESR by alternately optimizing the variables \mathcal{U} , \mathcal{V} , $\mathcal{D}, \mathcal{P}, \mathcal{Q}, \tilde{\mathbf{w}}$ and ϕ . Note that the globally optimal solution of the problem in (54) can be obtained at each iteration. Hence, the convergence of Algorithm 2 is guaranteed.
- 2) Complexity Analysis: The complexity of optimizing the auxiliary variables \mathcal{U} , \mathcal{V} , \mathcal{D} , \mathcal{P} and \mathcal{Q} is discussed first.

The complexity order for computing each \mathbf{u}_k in (32), v_k in (33), d_k in (37), \mathbf{p}_w in (40), \mathbf{p}_ϕ in (43), \mathbf{q}_w in (41), and \mathbf{Q}_ϕ in (44) is given by $\mathcal{O}(N^2K + N^2(M+1) + M^2N)$, $\mathcal{O}(N^2K + M^2N)$ $N^{2}(M+1)+K(M+1)^{2}$, $\mathcal{O}(N^{2}K+N^{2}(M+1)+(M+1)^{2})$, $\mathcal{O}(N^2K + N^2(M+1)), \mathcal{O}(N^2K + N^2(M+1)), \mathcal{O}(N^2K^2 +$ $N^2(M+1)$) and $\mathcal{O}(N^2K+N^2(M+1))$, respectively. Thus, the total computational complexity for obtaining \mathcal{U} , \mathcal{V} , \mathcal{D} , \mathcal{P} and Q is $\mathcal{O}(K(N^2K^2+N^2(M+1)+K(M+1)^2+M^2N))$.

The computational complexity for calculating the main optimization variables corresponds to the complexity of solving the SOCP problems formulated in (54) and (64). According to [47], since the problem in (54) includes a power constraint and K rate constraints whose dimension is NK, the corresponding complexity is $\mathcal{O}(N^3K^{5.5})$. Similarly, the relaxed version of the problem in (64) includes 2K rate constraints of dimension M and M constant modulus constraints of dimension one. Denoting by $t_{\rm max}$ the maximum number of iterations for Algorithm 1 to converge, the corresponding complexity is $\mathcal{O}\left(t_{\max}(M^{3.5}+M^3K^{2.5}+N^3K^{5.5})\right)$.

In summary, the computational complexity of each iteration of Algorithm 2 is $\mathcal{O}(t_{\text{max}}(M^{3.5} + M^3K^{2.5} + N^3K^{5.5}))$.

IV. BCD-MM ALGORITHM

In Algorithm 2, the use of CVX to solve the SOCP problems results in a large computational complexity, since high complexity optimization algorithms, such as the interior point method, are utilized. To reduce the computational complexity, we introduce, a BCD-MM algorithm. Specifically, since the objective functions in (51) and (60) are non-differentiable, we first derive smooth lower bound functions, and then apply the MM algorithm by introducing surrogate objective functions for the obtained lower bounds. We show that this approach results in a simple closed-form solution.

A. Approximates Functions

Based on [48], we approximate the objective functions in problems (51) and (60) as

$$\min_{k \in \mathcal{K}} \left\{ \tilde{r}_{\mathbf{w},k} \left(\tilde{\mathbf{w}} \right) \right\} \approx f \left(\tilde{\mathbf{w}} \right) = -\frac{1}{\zeta} \log \left(\sum_{k=1}^{K} \exp \left\{ -\zeta \tilde{r}_{\mathbf{w},k} \left(\tilde{\mathbf{w}} \right) \right\} \right), \tag{65}$$

$$\min_{k \in \mathcal{K}} \left\{ \tilde{r}_{\phi,k} \left(\phi \right) \right\} \approx f \left(\phi \right) = -\frac{1}{\zeta} \log \left(\sum_{k=1}^{K} \exp \left\{ -\zeta \tilde{r}_{\phi,k} \left(\phi \right) \right\} \right), \tag{66}$$

where $f(\tilde{\mathbf{w}})$ and $f(\phi)$ are lower bounds for the objective functions in (51) and (60), respectively, and $\zeta > 0$ is a smoothing parameter that satisfies the conditions:

$$f\left(\tilde{\mathbf{w}}\right) + \frac{1}{\zeta}\log\left(K\right) \geqslant \min_{k \in \mathcal{K}} \left\{\tilde{r}_{\mathbf{w},k}\left(\tilde{\mathbf{w}}\right)\right\} \geqslant f\left(\tilde{\mathbf{w}}\right) \quad (67)$$

$$f(\phi) + \frac{1}{\zeta} \log(K) \geqslant \min_{k \in \mathcal{K}} \{\tilde{r}_{\phi,k}(\phi)\} \geqslant f(\phi).$$
 (68)

In [49], the authors proved that $-\frac{1}{\mu}\log(\sum_{x\in\mathcal{X}}\exp\{-\mu x\})$ is a concave function of x and is monotonically increasing. Additionally, $\tilde{r}_{w,k}\left(\tilde{\mathbf{w}}\right)$ is a quadratic concave function of $\tilde{\mathbf{w}}$, and hence $f(\tilde{\mathbf{w}})$ is a concave function of $\tilde{\mathbf{w}}$. Similarly, $f(\phi)$ is a concave function of ϕ . The smoothing parameter ζ is optimized as described in [6]. Specifically, we set ζ equal to a small initial value, and then gradually increases it, to improve the approximation accuracy, until it reaches an upper limit $\zeta_{\rm max}.$ The advantage of this strategy is that it avoids local minima in the early stages of operation and avoids the loss of accuracy caused by the use of a large smoothing factor, which can degrade the performance of the MM algorithm.

B. Majorization-Minimization Method

Armed with the approximated functions in (65) and (66), we adopt the MM algorithm [50]. The MM algorithm does not directly optimize the functions in (65) and (66), but it operates on surrogate functions that are easier to optimize. Specifically, let us consider the maximization of the complex function $f(\mathbf{x})$ where \mathbf{x} belongs to a set $\mathcal{S}_{\mathbf{x}}$. Let us consider the surrogate function $\tilde{f}(\mathbf{x}|\mathbf{x}^{(n)})$ with given $\mathbf{x}^{(n)}$, where $\mathbf{x}^{(n)}$ is the optimal solution that corresponds to the surrogate function at the (n-1)-th iteration. The surrogate function $\hat{f}(\mathbf{x}|\mathbf{x}^{(n)})$ is said to minorize $f(\mathbf{x})$ at the given point $\mathbf{x}^{(n)}$ if the following conditions are satisfied [50]:

(A1) $\tilde{f}(\mathbf{x}|\mathbf{x}^{(n)})$ is continuous in \mathbf{x} and $\mathbf{x}^{(n)}$;

(A2) $\tilde{f}(\mathbf{x}^{(n)}|\mathbf{x}^{(n)}) = f(\mathbf{x}^{(n)}), \mathbf{x}^{(n)} \in \mathcal{S}_{\mathbf{x}};$

(A3) $\tilde{f}(\mathbf{x}|\mathbf{x}^{(n)}) \leqslant f(\mathbf{x}), \mathbf{x}, \mathbf{x}^{(n)} \in \mathcal{S}_{\mathbf{x}};$ (A4) $\tilde{f}'(\mathbf{x}^{(n)}|\mathbf{x}^{(n)};\eta)|_{\mathbf{x}=\mathbf{x}^{(n)}} = f'(\mathbf{x}^{(n)};\eta), \eta \text{ with } \mathbf{x}^{(n)} + \eta \in$ $S_{\mathbf{x}}$, where $f'(\mathbf{x}^{(n)}; \eta)$ is the directional derivative of $f(\mathbf{x}^{(n)})$,

$$f'(\mathbf{x}^{(n)};\eta) = \lim_{\lambda \to 0} \frac{f\left(\mathbf{x}^{(n)} + \lambda \eta\right) - f\left(\mathbf{x}^{(n)}\right)}{\lambda}.$$
 (69)

A drawback of the MM algorithm is that it may need many iterations to converge. To circumvent this issue, the SQUAREM method [51] is used to accelerate the convergence of the MM algorithm and hence to reduce the computational overhead.

C. Optimization of the Precoding Vector $\tilde{\mathbf{w}}$

With $f(\tilde{\mathbf{w}})$ defined in (65), the subproblem in (51) can be transformed into the following problem

$$\max_{\tilde{\mathbf{v}}} f(\tilde{\mathbf{w}}) \tag{70a}$$

s.t.
$$\tilde{\mathbf{w}} \in \mathcal{S}_{\tilde{\mathbf{w}}}$$
. (70b)

A surrogate function for $f(\tilde{\mathbf{w}})$ is given in the following lemma. Lemma 5: Let $\tilde{\mathbf{w}}^{(n)}$ be the solution at the (n-1)th iteration. For any feasible $\tilde{\mathbf{w}}$, $f(\tilde{\mathbf{w}})$ is minorized by the following quadratic function

$$\bar{f}\left(\tilde{\mathbf{w}}|\tilde{\mathbf{w}}^{(n)}\right) = \bar{c}_{w} + 2\operatorname{Re}\left\{\bar{\mathbf{v}}_{w}^{H}\tilde{\mathbf{w}}\right\} + \bar{\alpha}\tilde{\mathbf{w}}^{H}\tilde{\mathbf{w}},$$
 (71)

$$\bar{\mathbf{v}}_{\mathbf{w}} \triangleq \sum_{k=1}^{K} h_{\mathbf{w},k} \left(\tilde{\mathbf{w}}^{(n)} \right) \left(\tilde{\boldsymbol{b}}_{\mathbf{w},k} - \tilde{\mathbf{C}}_{\mathbf{w},k}^{\mathbf{H}} \tilde{\mathbf{w}}^{(n)} \right) - \bar{\alpha} \tilde{\mathbf{w}}^{(n)}, \quad (72a)$$

$$\bar{c}_{\mathbf{w}} \triangleq f\left(\tilde{\mathbf{w}}^{(n)}\right) + \bar{\alpha}\tilde{\mathbf{w}}^{(n),\mathrm{H}}\tilde{\mathbf{w}}^{(n)}$$
 (72b)

$$-2\operatorname{Re}\left\{ \sum_{k=1}^{K} h_{\mathrm{w},k} \left(\tilde{\mathbf{w}}^{(n)} \right) \left(\tilde{\boldsymbol{b}}_{\mathrm{w},k}^{\mathrm{H}} - \tilde{\mathbf{w}}^{(n),\mathrm{H}} \tilde{\mathbf{C}}_{\mathrm{w},k} \right) \tilde{\mathbf{w}}^{(n)} \right\},$$

$$\bar{\alpha} \triangleq -\max_{k} \left\{ \operatorname{Tr} \left[\tilde{\mathbf{C}}_{\mathbf{w},k} \right] \right\} - 2\zeta \max_{k} \left\{ \bar{o}_{\mathbf{w},k} \right\},$$
 (72c)

and $h_{\mathrm{w},k}\left(\mathbf{\tilde{w}}^{(n)}\right)$ and $\bar{o}_{\mathrm{w},k}$ are, respectively, given by

$$h_{\mathbf{w},k}\left(\mathbf{\tilde{w}}^{(n)}\right)$$

$$\triangleq \frac{\exp\left\{-\zeta \tilde{r}_{\mathbf{w},k}\left(\tilde{\mathbf{w}}^{(n)}\right)\right\}}{\sum_{k=1}^{K} \exp\left\{-\zeta \tilde{r}_{\mathbf{w},k}\left(\tilde{\mathbf{w}}^{(n)}\right)\right\}},\tag{73a}$$

$$\bar{o}_{\mathbf{w},k} \triangleq P \operatorname{Tr} \left[\tilde{\mathbf{C}}_{\mathbf{w},k} \tilde{\mathbf{C}}_{\mathbf{w},k}^{\mathrm{H}} \right] + \left\| \tilde{\boldsymbol{b}}_{\mathbf{w},k} \right\|_{2}^{2} + 2 \sqrt{P} \left\| \tilde{\mathbf{C}}_{\mathbf{w},k} \tilde{\boldsymbol{b}}_{\mathbf{w},k} \right\|_{2}.$$
(73b)

Proof: See Appendix A.

Therefore, the problem in (70) can be approximated as

$$\max_{\tilde{\mathbf{w}}} \bar{f}\left(\tilde{\mathbf{w}}|\tilde{\mathbf{w}}^{(n)}\right),\tag{74a}$$

$$s.t.\tilde{\mathbf{w}} \in \mathcal{S}_{\tilde{\mathbf{w}}}.$$
 (74b)

The optimization problem in (74) can be solved by using the method of Lagrangian multipliers. Specifically, the Lagrangian function is given by

$$L\left(\tilde{\mathbf{w}},\varepsilon\right) = \bar{f}\left(\tilde{\mathbf{w}}|\tilde{\mathbf{w}}^{(n)}\right) - \varepsilon\left(\tilde{\mathbf{w}}^{\mathrm{H}}\tilde{\mathbf{w}} - P\right),\tag{75}$$

where ε is the Lagrange multiplier. Therefore, the optimal solution $\tilde{\mathbf{w}}$ of the surrogate optimization problem in (75) at the n-th iteration is

$$\tilde{\mathbf{w}}^{(n+1)} = -\sqrt{\frac{P}{\bar{\mathbf{v}}_{w}^{H}\bar{\mathbf{v}}_{w}}}\bar{\mathbf{v}}_{w}.$$
 (76)

D. Optimization of the Vector ϕ of Reflection Coefficients

With $f(\phi)$ defined in (66), the subproblem in (60) can be transformed into the following problem

$$\max_{\perp} f(\phi) \tag{77a}$$

s.t.
$$\phi \in \mathcal{S}_{\phi}$$
. (77b)

A surrogate function for $f(\phi)$ is given in the following lemma.

Lemma 6: Let $\phi^{(n)}$ be the solution at the (n-1)-th iteration. For any feasible ϕ , $f(\phi)$ is minorized by the following function

$$\bar{f}\left(\phi|\phi^{(n)}\right) = \bar{c}_{\phi} + 2\operatorname{Re}\left\{\bar{\mathbf{v}}_{\phi}^{H}\phi\right\},$$
 (78)

where n is the iteration number, and

$$\bar{\mathbf{v}}_{\phi} \triangleq \sum_{k=1}^{K} h_{\phi,k} \left(\boldsymbol{\phi}^{(n)} \right) \left(\tilde{\boldsymbol{b}}_{\phi,k} - \tilde{\mathbf{C}}_{\phi,k}^{\mathrm{H}} \boldsymbol{\phi}^{(n)} \right) - \bar{\beta} \boldsymbol{\phi}^{(n)}, \quad (79a)$$

$$\bar{c}_{\phi} \triangleq \bar{f}\left(\phi^{(n)}\right) + 2M\bar{\beta}$$
 (79b)

$$-2\operatorname{Re}\left\{\sum_{k=1}^{K}h_{\phi,k}\left(\boldsymbol{\phi}^{(n)}\right)\left(\tilde{\boldsymbol{b}}_{\phi,k}^{H}-\boldsymbol{\phi}^{n,H}\tilde{\mathbf{C}}_{\phi,k}\right)\boldsymbol{\phi}^{(n)}\right\},\right.$$

$$h_{\phi,k}\left(\boldsymbol{\phi}^{(n)}\right) \triangleq \frac{\exp\left\{-\zeta\tilde{r}_{\phi,k}\left(\boldsymbol{\phi}^{(n)}\right)\right\}}{\sum_{k=1}^{K}\exp\left\{-\zeta\tilde{r}_{\phi,k}\left(\boldsymbol{\phi}^{(n)}\right)\right\}},$$

$$\bar{\beta} \triangleq -\max_{k}\left\{\lambda_{\max}\left(\tilde{\mathbf{C}}_{\phi,k}\right)\right\}$$

$$-2\zeta\max_{k}\left\{\left\|\tilde{\boldsymbol{b}}_{\phi,k}\right\|_{2}^{2} + M\lambda_{\max}\left(\tilde{\mathbf{C}}_{\phi,k}\tilde{\mathbf{C}}_{\phi,k}^{\mathbf{H}}\right)\right\}$$
(80a)

Proof: See [43, Appendix D].

Therefore, the problem in (77) can be approximated as

$$\max_{\phi} \bar{f}\left(\phi|\phi^{(n)}\right) \tag{81a}$$

 $+2 \|\tilde{\mathbf{C}}_{\phi,k}\tilde{\boldsymbol{b}}_{\phi,k}\|_{_{1}}$.

s.t.
$$\phi \in \mathcal{S}_{\phi}$$
. (81b)

The optimal solution $\phi^{(n+1)}$ at the *n*-th iteration is given by $\boldsymbol{\phi}^{(n+1)} = \exp\left\{j\angle \bar{\mathbf{v}}_{\phi}\right\},\,$ (82)

where $\exp(\cdot)$ and $\angle(\cdot)$ are intended as element-wise functions.

E. Algorithm Development

1) BCD-MM Algorithm: The accelerated version of the BCD-MM algorithm is summarized in Algorithm 3. Specifically, the optimization problems in (51) and (60) are transformed into the optimization problems in (74) and (81), whose approximate optimal solutions are given in (76) and (82), respectively. In Algorithm 3, the following notation is used: $\mathcal{R}(\cdot)$ is the objective function of the problem in (23); $\mathcal{F}_{w}(\cdot)$ and $\mathcal{F}_{\phi}(\cdot)$ denote the nonlinear fixed-point iteration map of the MM algorithm in (76) and (82), respectively. Specifically, steps 6 and 11 refer to the proposed gradient method based on the SQUAREM method. Steps 7 and 12 refer to the projection operation to force wayward points to satisfy the nonlinear constraints. In addition, steps 8 and 13 ensure the ascent property of Algorithm 3. In step 14, the adjustment factor ι is used to successively increase the smoothness factor ζ from its initial value to ζ_{\max} .

2) Convergence Analysis: Since the surrogate function $\bar{f}\left(\tilde{\mathbf{w}}|\tilde{\mathbf{w}}^{(n)}\right)$ satisfies the conditions $\bar{f}\left(\tilde{\mathbf{w}}|\tilde{\mathbf{w}}^{(n)}\right) \leqslant f\left(\tilde{\mathbf{w}}\right)$, and $\bar{f}(\tilde{\mathbf{w}}^{(n)}|\tilde{\mathbf{w}}^{(n)}) = f(\tilde{\mathbf{w}}^{(n)}), \text{ with given } \phi^{(n)}, \text{ we have }$

$$f(\tilde{\mathbf{w}}^{(n)}, \boldsymbol{\phi}^{(n)}) = \bar{f}(\tilde{\mathbf{w}}^{(n)} | \tilde{\mathbf{w}}^{(n)}) \leqslant \bar{f}(\tilde{\mathbf{w}}^{(n+1)} | \tilde{\mathbf{w}}^{(n)})$$

$$\leqslant f(\tilde{\mathbf{w}}^{(n+1)}, \boldsymbol{\phi}^{(n)}). \tag{83}$$

Similarly, with given $\tilde{\mathbf{w}}^{(n)}$, we have

$$f(\phi^{(n)}, \tilde{\mathbf{w}}^{(n+1)}) = \bar{f}(\phi^{(n)}|\phi^{(n)}) \leqslant \bar{f}(\phi^{(n+1)}|\phi^{(n)}) \leqslant f(\phi^{(n+1)}, \tilde{\mathbf{w}}^{(n+1)}).$$
(84)

Algorithm 3 BCD-MM Algorithm

Initialize: Initialize $\tilde{\mathbf{w}}^{(0)}$, $\phi^{(0)}$ to feasible values. Set n=0, the smoothing factor ζ , the maximum value of the smoothing factor ζ_{max} , the adjustment factor ι , the maximum number of iterations n_{\max} and the error tolerance ε .

1: while
$$\varepsilon \leqslant \left| \mathcal{R}(\tilde{\mathbf{w}}^{(n+1)}, \phi^{(n+1)}) - \mathcal{R}\left(\tilde{\mathbf{w}}^{(n)}, \phi^{(n)}\right) \right|$$

$$/ \left| \mathcal{R}\left(\tilde{\mathbf{w}}^{(n)}, \phi^{(n)}\right) \right| \text{ and } n \leqslant n_{\max} \text{ do}$$
2: Given $\tilde{\mathbf{w}}^{(n)}$ and $\phi^{(n)}$, calculate $\mathcal{U}^{(n+1)}$, $\mathcal{V}^{(n+1)}$, $\mathcal{D}^{(n+1)}$, $\mathcal{D}^{(n+1)}$ and $\mathcal{Q}^{(n+1)}$ by using (32), (33), (37), (40), (43), (41) and (44);
3: Calculate $\tilde{\mathbf{w}}_1 = \mathcal{F}_{\mathbf{w}}\left(\tilde{\mathbf{w}}^{(n)}\right)$ and $\tilde{\mathbf{w}}_2 = \mathcal{F}_{\mathbf{w}}\left(\tilde{\mathbf{w}}_1\right)$;
4: Calculate $\tilde{\mathbf{j}}_1 = \tilde{\mathbf{w}}_1 - \tilde{\mathbf{w}}^{(n)}$ and $\tilde{\mathbf{j}}_2 = \tilde{\mathbf{w}}_2 - \tilde{\mathbf{w}}_1 - \tilde{\mathbf{j}}_1$;
5: Calculate the step factor $\alpha = -\frac{\|\tilde{\mathbf{j}}_1\|_2}{\|\tilde{\mathbf{j}}_2\|_2}$;
6: Calculate $\tilde{\mathbf{w}}^{(n+1)} = \tilde{\mathbf{w}}^{(n)} - 2\alpha\tilde{\mathbf{j}}_1 + \alpha^2\tilde{\mathbf{j}}_2$;
7: If $\left\| \tilde{\mathbf{w}}^{(n+1)} \right\|_2 > \sqrt{P}$, set $\tilde{\mathbf{w}}^{(n+1)} \leftarrow \frac{\sqrt{P}}{\|\tilde{\mathbf{w}}^{(n+1)}\|_2} \tilde{\mathbf{w}}^{(n+1)}$;
8: If $f\left(\tilde{\mathbf{w}}^{(n+1)}\right) < f\left(\tilde{\mathbf{w}}_2\right)$, set $\alpha \leftarrow \frac{(\alpha-1)}{2}$, go back to step 3;
9: Calculate $\phi_1 = \mathcal{F}_{\phi}\left(\phi^{(n)}\right)$ and $\phi_2 = \mathcal{F}_{\phi}\left(\phi_1\right)$;
10: Calculate $\mathbf{k}_1 = \phi_1 - \phi^{(n)}$ and $\mathbf{k}_2 = \phi_2 - \phi_1 - \mathbf{k}_1$;
11: Calculate the step factor $\beta = -\frac{\|\mathbf{k}_1\|_2}{\|\mathbf{k}_2\|_2}$;
12: Calculate $\phi^{(n+1)} = \exp\left\{ \angle\left(\phi^{(n)} - 2\beta\mathbf{k}_1 + \beta^2\mathbf{k}_2\right) \right\}$;
13: If $f\left(\phi^{(n+1)}\right) < f\left(\phi_2\right)$, set $\beta \leftarrow \frac{(\beta-1)}{2}$, go back to step 9;
14: Set $\zeta \leftarrow \min\left(\zeta^{\iota}, \zeta_{\max}\right)$ and $n \leftarrow n + 1$;

Then, the values of the objective function generated by the BCD-MM algorithm are monotonically increasing. In addition, subject to the maximum transmit power constraint, the objective function in (23) is upper bounded. Hence, the BCD-MM algorithm is guaranteed to converge.

3) Complexity Analysis: The computational complexity of optimizing the variables \mathcal{U} , \mathcal{V} , \mathcal{D} , \mathcal{P} and \mathcal{Q} is the same as in Section III-D, which is $\mathcal{O}(K(N^2K^2 + N^2(M+1) +$ $K(M+1)^2 + M^2N$). Therefore, we are left with the analysis of the computational complexity of the two remaining optimization variables $\tilde{\mathbf{w}}$ and ϕ . First, we note that $\tilde{r}_{\mathrm{w},k}\left(\mathbf{\tilde{w}}^{(n)}\right)$ and $\tilde{r}_{\phi,k}\left(\mathbf{\tilde{w}}^{(n)}\right)$ can be reused when calculating $h_{\mathrm{w},k}\left(\mathbf{\tilde{w}}^{(n)}\right)$ and $h_{\phi,k}\left(\mathbf{\tilde{w}}^{(n)}\right)$, respectively. Also, we note that the complexity required to calculate $h_{\mathbf{w},k}\left(\tilde{\mathbf{w}}^{(n)}\right)$ and $h_{\phi,k}(\tilde{\mathbf{w}}^{(n)})$ is $\mathcal{O}(K(N^2K^2+N^2(M+1)+M^2N))$ and $\mathcal{O}\left(K\left(N^2K+N^2\left(M+1\right)+M^2N\right)\right)$, respectively.

As far as the optimization of $\tilde{\mathbf{w}}$ is concerned, the complexity of computing $\bar{o}_{w,k}$ and $\bar{\alpha}$ is $\mathcal{O}(N^3K^3)$ and $\mathcal{O}(K(N^3K^3))$, respectively. The complexity of calculating $\bar{\mathbf{v}}_{\mathrm{w}}$ mainly depends on $h_{\mathbf{w},k}\left(\tilde{\mathbf{w}}^{(n)}\right)$. Hence, the complexity of computing $\tilde{\mathbf{w}}^{(n+1)}$ is $\mathcal{O}(K(N^3K^3 + N^2(M+1) + M^2N))$. As far as the computational complexity of the subproblems corresponding to ϕ is concerned, the complexity of computing $\lambda_{\max} \left(\tilde{\mathbf{C}}_{\phi,k} \tilde{\mathbf{C}}_{\phi,k}^{\mathrm{H}} \right)$ is $\mathcal{O}(M^3)$ and the complexity required to find $\bar{\beta}$ is $\mathcal{O}(K(M^3 +$ $N^2K+N^2(M+1)+M^2N)$). Hence, the complexity of calculating $\phi^{(n+1)}$ is $\mathcal{O}(K(M^3+N^2K+N^2(M+1)+N^2(M+1))$

Finally, the computational complexity of each iteration of Algorithm 2 is $\mathcal{O}(K(N^3K^3 + M^3 + N^2(M+1) + M^2N))$. Therefore, the complexity of Algorithm 3 is lower than that of Algorithm 2.

14:

15: end while

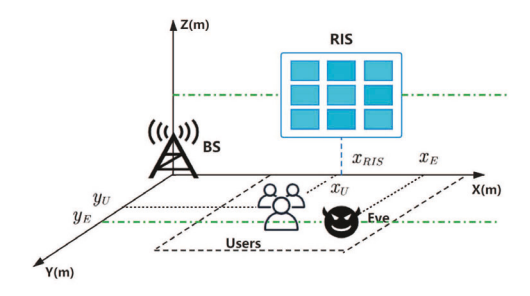


Fig. 2. The simulated RIS-assisted MISO communication scenario.

V. SIMULATION RESULTS

A. Simulation Setup

In this section, simulation results are illustrated to evaluate the performance of the proposed BCD-SOCP and BCD-MM algorithms. Figure 2 depicts the considered simulation setup, wherein the BS and the RIS are located at (0 m, 0 m, 30 m) and ($x_{\rm RIS}$, 0 m, 10 m), respectively. Unless stated otherwise, $x_{\rm RIS} = 50$ m. Three legitimate users are randomly located in a 10 m \times 10 m area, whose center is ($x_{\rm U}$, $y_{\rm U}$, 1.5 m), and the eavesdropper is located at ($x_{\rm E}$, $y_{\rm E}$, 1.5 m). We assume that $x_{\rm U} = x_{\rm E} = 300$ m and $y_{\rm U} = y_{\rm E} = 10$ m. In addition, unless stated otherwise, the number of BS transmit antennas and RIS reflecting elements is N=4 and M=16, respectively.

The large-scale path loss is defined as

$$PL = -30 - 10\alpha \log_{10} d, \tag{85}$$

where α is the path loss exponent and d is the link distance in meters. The path loss exponents of the BS-RIS channel, RIS-user channel, RIS-eavesdropper channel, BS-user channel and BS-eavesdropper channel are equal to $\alpha_{\rm BR}=\alpha_{\rm RU}=\alpha_{\rm RE}=2$ and $\alpha_{\rm BU}=\alpha_{\rm BE}=4$, respectively.

We assume a rich scattering environment. Therefore, the small scale fading of the BS-user channel and BS-eavesdropper channel is assumed to be Rayleigh fading. In addition, the small scale fading of the RIS-related channels is assumed to obey a Rician distribution, and, therefore, the channel is

$$\tilde{\mathbf{H}} = \sqrt{\frac{\kappa}{\kappa + 1}} \tilde{\mathbf{H}}^{\text{LoS}} + \sqrt{\frac{1}{\kappa + 1}} \tilde{\mathbf{H}}^{\text{NLoS}}, \tag{86}$$

where κ is the Rician factor, $\tilde{\mathbf{H}}^{\mathrm{LoS}}$ and $\tilde{\mathbf{H}}^{\mathrm{NLoS}}$ denote the line-of-sight (LoS) and the non-line-of-sight (NLoS) components, respectively. $\tilde{\mathbf{H}}^{\mathrm{LoS}}$ is defined as the product of the steering vectors of the transmitter and receiver, while $\tilde{\mathbf{H}}^{\mathrm{NLoS}}$ is randomly generated according to a Rayleigh distribution with unit power. Unless stated otherwise, we set $\kappa=10$.

The MOSEK solver [52] in the CVX toolbox is used to solve the SOCP problem in Algorithm 2. The final results are obtained by averaging over 200 independent channels. Unless stated otherwise, the simulation parameters are set as follows: the HI factors are $\kappa_{\rm t}=\kappa_{\rm r,k}=0.01$, the BS transmit power is P=1 W, the channel bandwidth is 10 MHz, the weighting factors are $\omega_k=1$, the noise power density is -174 dBm/Hz, the initial smoothing parameter is $\zeta=1.25$, the adjustment factor is $\iota=1.02$, the upper limit of the smoothing parameter is $\zeta_{\rm max}=500$, and the error tolerance is

 $\varepsilon=10^{-5}$. Each element of the reflection coefficient vector ϕ is initialized by uniformly and randomly selecting the phase shift in $[0,2\pi]$. The precoding matrix \mathbf{W} is initialized by extracting the real and imaginary parts of each element of W from an independent Gaussian distribution, and then scaling \mathbf{W} to satisfy the constraint $\mathrm{Tr}(\mathbf{W}^H\mathbf{W}) \leqslant P$.

B. Baseline Schemes

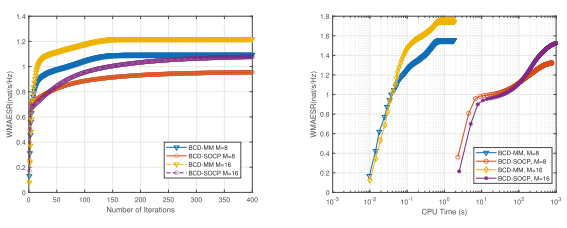
We compare the performance of the proposed algorithms with the following baseline schemes.

- To verify the effectiveness of the proposed robust design, we implement a **Non-Robust** version of the proposed approach that ignores the HIs at both the RIS and the transceiver.
- 2) To analyze the benefits of deploying an RIS in term of improving the security of a communication system, we consider a scenario without the RIS and optimize only the precoding vector w by applying the BCD-MM algorithm. The corresponding algorithm is referred to as BCD-MM-No-RIS.
- 3) To study the advantages of jointly optimizing the precoding at the BS and the phase shifts at the RIS, we consider a scheme in which only $\tilde{\mathbf{w}}$ is optimized and the reflection coefficient vector $\boldsymbol{\phi}$ is set randomly. The corresponding algorithm is referred to as **BCD-MM-Rand**.
- 4) To verify the effectiveness of the proposed MM algorithm for solving the subproblem of ϕ , we consider a **BCD-MM-SDR** version of the proposed approach that uses the SDR [53] method to optimize ϕ .
- 5) In practice, it may be difficult and expensive to implement RISs that are capable of adjusting the phase shifts to any arbitrary continuous value. Therefore, we study the performance of Algorithm 2 when the phase shifts of the RIS are quantized with two bits, i.e., only four phase shifts can be realized. The corresponding scheme is referred to as **BCD-MM-2bit**. Specifically, let ϕ_m^{con} be the optimal phase shift of the m-th element of the RIS, which is obtained by applying the **BCD-MM** algorithm. Then, the corresponding 2-bit quantized phase shift is

$$\phi_m^{dis} = \exp\left\{\arg\min_{\theta} \left| \angle \phi_m^{con} - \theta \right| \right\}, \qquad (87)$$
where $\theta \in \left\{0, \frac{\pi}{2}, \pi, \frac{3\pi}{2}\right\}.$

C. Convergence Behavior of the Proposed Algorithms

Figure 3 illustrates the convergence behavior of the two proposed algorithms as a function of the number of RIS elements M. We see that the **BCD-MM** algorithm converges within 150 iterations, while the **BCD-SOCP** algorithm converges within 350 iterations. Compared with the **BCD-SOCP** algorithm, the **BCD-MM** algorithm converges to a larger value of the WMAESR, but it requires less CPU time, which confirms the superiority of the **BCD-MM** algorithm. In addition, the obtained results show that the **BCD-MM** algorithm converges in almost the same number of iterations and CPU time for different values of M. This is mainly because the convergence speed of the MM algorithm is closely related to



(a) Achievable WMAESR versus the (b) Achievable WMAESR versus the number of iterations CPU time

Fig. 3. Convergence behavior of the proposed algorithms for M = [8, 16].

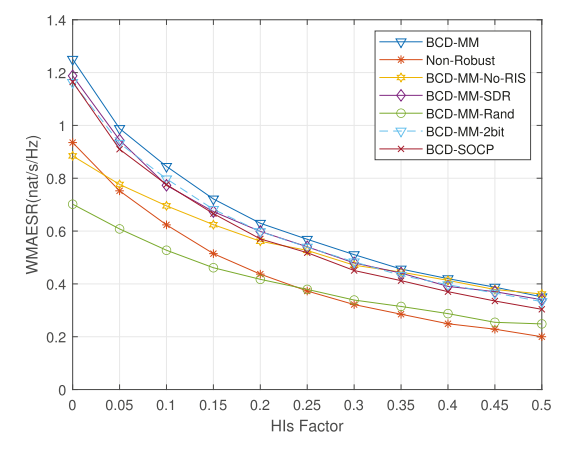


Fig. 4. Achievable WMAESR versus the HIs factor.

the approximation accuracy of the surrogate function, which is affected by the strategy for updating the smoothing factor.

D. Impact of the HIs Factor

The impact of the HIs factor is shown in Figure 4. We see that the security performance of the **Non-Robust** and **BCD-MM** algorithms degrades as the HIs factor increases. However, as the HIs factor increases, the WMAESR of the **BCD-MM** algorithm always outperforms the **Non-Robust** algorithm, which demonstrates the strength of the proposed robust transmission design. Since the **BCD-MM-Rand** algorithm does not attempt to optimize the phase shifts of the RIS, it offers the worst security performance, which highlights the superiority of the joint optimization strategy. In addition, we see that the security performance of the **BCD-SOCP** algorithm is always worse than that of the **BCD-MM** algorithm, which further corroborates the superiority of the **BCD-MM** algorithm compared with the **BCD-SOCP** algorithm.

E. Impact of the Maximum Transmit Power

Figure 5 illustrates the impact of the maximum transmit power on the WMAESR. In this context, it is worth recalling that the distortion noise at the transceiver is assumed to be proportional to the signal power. Hence, increasing the signal power improves the SNR, but it increases the performance loss caused by the presence of HIs as well. We see that the security performance gap between the **Non-Robust** and the **BCD-MM** algorithms gradually increases as the transmit power increases. This is because the **Non-Robust** algorithm does not account for the HIs by design, and its performance degradation is more prominent. Additionally, we see that the WMAESR of the **Non-Robust** algorithm gradually decreases

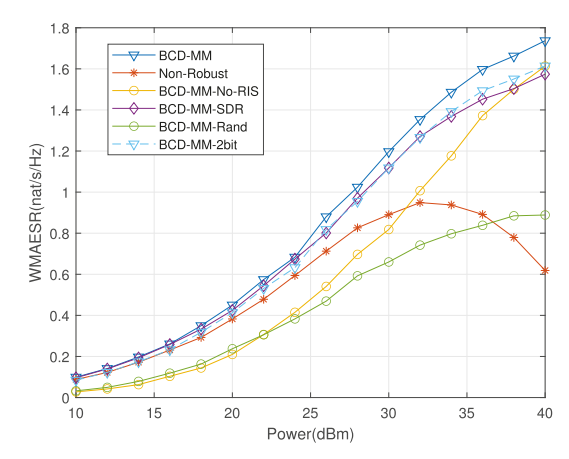


Fig. 5. Achievable WMAESR versus the maximum transmit power.

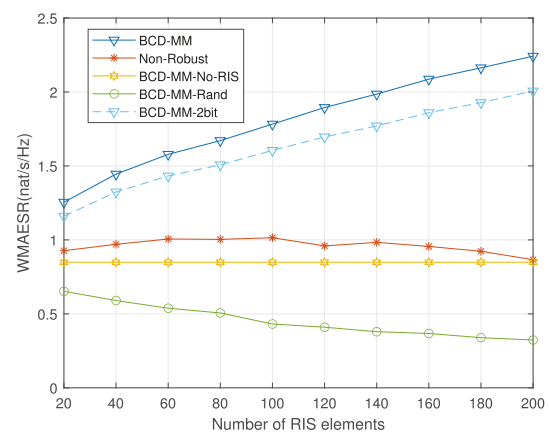


Fig. 6. Achievable WMAESR versus the number of RIS elements M.

when the transmit power is greater than 32 dBm, which further strengthen the necessity of designing robust algorithms in the high transmit power regime. Furthermore, we see that the security performance of the **BCD-MM** algorithm is always better than the **BCD-MM-SDR** algorithm, which substantiates the superiority of the proposed MM algorithm for solving the subproblem of the reflection coefficient vector ϕ over the SDR method.

F. Impact of the Number of RIS Elements

Figure 6 illustrates the WMAESR as a function of the number of RIS elements. As expected, increasing the number of RIS elements improves the AESR. We can also see a diminishing return law as a function of the RIS elements. However, this diminishing return law is not very significant for the proposed **BCD-MM** algorithm in the range of Mfrom 20 to 200, which illustrates the effectiveness of our algorithm as the number of RIS elements increases. However, the WMAESR of the Non-Robust and BCD-MM-Rand algorithms is significantly lower than that of the BCD-MM-2bit algorithm, which further corroborates the advantages of the proposed robust design against the HIs. Furthermore, the WMAESR of the BCD-MM-No-RIS algorithm is much lower than that of the BCD-MM-2bit algorithm, which demonstrates the potential benefits of deploying an RIS for enhancing the secrecy rate.

VI. CONCLUSION

In this paper, we studied the AESR of an RIS-aided multiuser wireless network in the presence of hardware impairments. We demonstrated that the deployment of an RIS can effectively increase the AESR of the legitimate users through appropriate adjustment of the RIS phase shifts and the precoding matrix of the BS. We introduced a BCD framework for jointly optimizing the precoding at the BS and the phase shifts of the RIS. Specifically, we decoupled the original problem into two tractable subproblems and proposed an SOCP-based algorithm to alternately optimize them. To reduce the computational complexity, we proposed an MM algorithm based on surrogate functions that are formulated in a closed-form expression. Simulation results demonstrated the advantages of the proposed robust transmission design that accounts for the hardware impairments by design, as well as the computational efficiency of the proposed solutions in terms of number of iterations and CPU time.

APPENDIX A PROOF OF LEMMA 5

Considering that the objective function $\tilde{r}_k(\tilde{\mathbf{w}})$ of the optimization problem in (51) is a quadratic function, we assume that there exists a minorizing function $f(\tilde{\mathbf{w}})$ satisfying the following quadratic form

$$\bar{f}\left(\tilde{\mathbf{w}}|\tilde{\mathbf{w}}^{(n)}\right) = f\left(\tilde{\mathbf{w}}^{(n)}\right) + 2\operatorname{Re}\left\{\mathbf{g}_{w}^{H}\left(\tilde{\mathbf{w}} - \tilde{\mathbf{w}}^{(n)}\right)\right\} \\
+ \left(\tilde{\mathbf{w}} - \tilde{\mathbf{w}}^{(n)}\right)^{H}\mathbf{M}_{w}\left(\tilde{\mathbf{w}} - \tilde{\mathbf{w}}^{(n)}\right), (88)$$

where $\mathbf{g}_{\mathrm{w}} \in \mathbb{C}^{NK \times 1}$ and $\mathbf{M}_{\mathrm{w}} \in \mathbb{C}^{NK \times NK}$ are parameters to be determined.

The function $\bar{f}(\tilde{\mathbf{w}})$ is a minorizing function if it fulfills the following conditions:

(C1) $\bar{f}(\tilde{\mathbf{w}}|\tilde{\mathbf{w}}^{(n)})$ is continuous in $\tilde{\mathbf{w}}$ and $\tilde{\mathbf{w}}^{(n)}$; (C2) $\bar{f}(\tilde{\mathbf{w}}^{(n)}|\tilde{\mathbf{w}}^{(n)}) = f(\tilde{\mathbf{w}}^{(n)}), \tilde{\mathbf{w}}^{(n)} \in \mathcal{S}_{\tilde{\mathbf{w}}};$ (C3) $\bar{f}(\tilde{\mathbf{w}}|\tilde{\mathbf{w}}^{(n)}) \leq f(\tilde{\mathbf{w}}), \tilde{\mathbf{w}}, \tilde{\mathbf{w}}^{(n)} \in \mathcal{S}_{\tilde{\mathbf{w}}};$ (C4) $\bar{f}'(\tilde{\mathbf{w}}^{(n)}|\tilde{\mathbf{w}}^{(n)};\eta)|_{\tilde{\mathbf{w}}=\tilde{\mathbf{w}}^{(n)}} = f'(\tilde{\mathbf{w}}^{(n)};\eta), \forall \eta \text{ with } \tilde{\mathbf{w}}^{(n)} +$ $\eta \in \mathcal{S}_{\tilde{\mathbf{w}}}$.

To this end, we derive \mathbf{g}_w and \mathbf{M}_w that satisfy the conditions (C1) - (C4). Since $\bar{f}(\tilde{\mathbf{w}})$ is a quadratic function, in addition, the condition (C1) is satisfied. By substituting $\tilde{\mathbf{w}}^{(n)}$ into $\bar{f}(\tilde{\mathbf{w}}|\tilde{\mathbf{w}}^{(n)})$, it can be verified that $\bar{f}(\tilde{\mathbf{w}})$ satisfies the condition (C2). Hence, \mathbf{g}_{w} and \mathbf{M}_{w} need to be determined in order to fulfill the conditions (C3) and (C4).

First, we derive an expression for g_w that fulfills (C4), which requires that the first-order derivatives of $f(\tilde{\mathbf{w}}^{(n)})$ and $\bar{f}(\tilde{\mathbf{w}}|\tilde{\mathbf{w}}^{(n)})$ are equal in any direction. Let $\tilde{\mathbf{w}}^m$ belongs to $S_{\mathbf{w}}$. The directional derivative of $f(\tilde{\mathbf{w}})$ in the direction $\tilde{\mathbf{w}}^{(m)} - \tilde{\mathbf{w}}^{(n)}$ is given by (89), shown at the bottom of the page, where $h_{w,k}(\tilde{\mathbf{w}}^{(n)})$ is defined in (73a). Moreover, the directional derivative of $\tilde{f}(\tilde{\mathbf{w}}|\tilde{\mathbf{w}}^{(n)})$ in (88) evaluated at $\tilde{\mathbf{w}}^{(n)}$ in the same direction is given by

$$2\operatorname{Re}\left\{\mathbf{g}_{w}^{H}\left(\tilde{\mathbf{w}}^{(m)}-\tilde{\mathbf{w}}^{(n)}\right)\right\}.$$
(90)

Therefore, the vector \mathbf{g}_{w} is derived as

$$\mathbf{g}_{\mathbf{w}} = \sum_{k=1}^{K} h_{\mathbf{w},k} \left(\tilde{\mathbf{w}}^{(n)} \right) \left(\tilde{\boldsymbol{b}}_{\mathbf{w},k} - \tilde{\mathbf{C}}_{\mathbf{w},k}^{\mathbf{H}} \tilde{\mathbf{w}}^{(n)} \right). \tag{91}$$

Then, we derive an expression for $M_{\rm w}$ that fulfills (C3). This requires that $\tilde{f}(\tilde{\mathbf{w}}|\tilde{\mathbf{w}}^{(n)})$ is a lower bound of $f(\tilde{\mathbf{w}})$ for each linear cut in any direction. Therefore, for any auxiliary variable $\eta \in [0,1]$ and $\tilde{\mathbf{w}}^{(m)} \in \mathcal{S}_{\mathrm{w}}$, \mathbf{M}_{w} needs to be chosen so that the following expression is fulfilled

$$f(\tilde{\mathbf{w}}^{(n)} + \eta(\tilde{\mathbf{w}}^{(m)} - \tilde{\mathbf{w}}^{(n)}))$$

$$\geqslant f(\tilde{\mathbf{w}}^{(n)}) + 2\eta \operatorname{Re} \left\{ \mathbf{g}_{w}^{H}(\tilde{\mathbf{w}} - \tilde{\mathbf{w}}^{(n)}) \right\}$$

$$+ \eta^{2} (\tilde{\mathbf{w}} - \tilde{\mathbf{w}}^{(n)})^{H} \mathbf{M}_{w} (\tilde{\mathbf{w}} - \tilde{\mathbf{w}}^{(n)}). \tag{92}$$

Let us define $\bar{m}_{\rm w}\left(\eta\right)$ and $\bar{n}_{\rm w}\left(\eta\right)$ as the left and right hand sides of (92), respectively. By inspection, we note that $\bar{m}_{w}(0)$ is equal to $\bar{n}_{w}(0)$. Also, the first-order derivative of $\bar{m}_{\mathrm{w}}(\eta)$ is given by $\nabla_{\eta}\bar{m}_{\mathrm{w}}(\eta) = \sum_{k=1}^{K} \hat{g}_{\mathrm{w},k}(\eta) \nabla_{\eta}\hat{h}_{\mathrm{w},k}(\eta)$, where $\nabla_{\eta}\hat{h}_{\mathrm{w},k}(\eta) = -2\eta \left(\tilde{\mathbf{w}}^{(m)} - \tilde{\mathbf{w}}^{(n)}\right)^{\mathrm{H}} \tilde{\mathbf{C}}_{\mathrm{w},k} \left(\tilde{\mathbf{w}}^{(m)} - \tilde{\mathbf{w}}^{(n)}\right) + 2\mathrm{Re}\left\{\tilde{\boldsymbol{b}}_{\mathrm{w},k}^{\mathrm{H}} \left(\tilde{\mathbf{w}}^{(m)} - \tilde{\mathbf{w}}^{(n)}\right) - \left(\tilde{\mathbf{w}}^{(n)}\right)^{\mathrm{H}} \tilde{\mathbf{C}}_{\mathrm{w},k} \left(\tilde{\mathbf{w}}^{(m)} - \tilde{\mathbf{w}}^{(n)}\right)\right\},$
$$\begin{split} \hat{h}_{\mathrm{w},k}\left(\eta\right) & \triangleq \tilde{r}_{\mathrm{w},k}\left(\tilde{\mathbf{w}}^{(n)} + \eta\left(\tilde{\mathbf{w}}^{(m)} - \tilde{\mathbf{w}}^{(n)}\right)\right) \quad \text{and} \\ \hat{g}_{\mathrm{w},k}\left(\eta\right) & \triangleq \frac{\exp\left\{-\zeta\hat{h}_{\mathrm{w},k}(\eta)\right\}}{\sum_{i=1}^{K}\exp\left\{-\zeta\hat{h}_{\mathrm{w},i}(\eta)\right\}}. \\ \text{It can be verified that } \nabla_{\eta}\bar{m}_{\mathrm{w}}\left(0\right) \text{ is equal to } \nabla_{\eta}\bar{n}_{\mathrm{w}}\left(0\right). \end{split}$$

Hence, we obtain the sufficient condition for (92), as follows

$$\nabla_{\eta}^{2} \bar{m}_{w}(\eta) \geqslant \nabla_{\eta}^{2} \bar{n}_{w}(\eta), \eta \in [0, 1]. \tag{93}$$

Next, we further manipulate (93) to solve for \mathbf{M}_{w} . To this end, we define $\mathbf{e}_k \triangleq \tilde{\boldsymbol{b}}_{\mathrm{w},k} - \tilde{\mathbf{C}}_{\mathrm{w},k}^{\mathrm{H}} \left(\tilde{\mathbf{w}}^{(n)} + \eta \left(\tilde{\mathbf{w}}^{(m)} - \tilde{\mathbf{w}}^{(n)} \right) \right)$ and $\bar{\mathbf{w}} \triangleq \tilde{\mathbf{w}}^{(m)} - \tilde{\mathbf{w}}^{(n)}$, so that $\nabla_{\eta}^2 \bar{\eta}_{\mathrm{w}} \left(\eta \right)$ can be derived as

$$\nabla_{\eta}^{2} \bar{n}_{w} (\eta) = 2 \left(\tilde{\mathbf{w}}^{(m)} - \tilde{\mathbf{w}}^{(n)} \right)^{H} \mathbf{M}_{w} \left(\tilde{\mathbf{w}}^{(m)} - \tilde{\mathbf{w}}^{(n)} \right)$$
$$= \left[\bar{\mathbf{w}}^{H} \ \bar{\mathbf{w}}^{T} \right] \begin{bmatrix} \mathbf{M}_{w} & 0 \\ 0 & \mathbf{M}_{w}^{T} \end{bmatrix} \begin{bmatrix} \bar{\mathbf{w}} \\ \bar{\mathbf{w}}^{*} \end{bmatrix}. \tag{94}$$

Similarly, $\nabla_{\eta}^2 \bar{m}_{\rm w}(\eta)$ is given 1

 $\nabla_{\eta}^2 \bar{m}_{\rm w} (\eta)$

$$= \sum_{k=1}^{K} \left(\hat{g}_{\mathbf{w},k} \left(\eta \right) \nabla_{\eta}^{2} \hat{h}_{\mathbf{w},k} \left(\eta \right) - \zeta \hat{g}_{\mathbf{w},k} \left(\eta \right) \left(\nabla_{\eta} \hat{h}_{\mathbf{w},k} \left(\eta \right) \right)^{2} \right) + \zeta \left(\sum_{k=1}^{K} \hat{g}_{\mathbf{w},k} \left(\eta \right) \nabla_{\eta} \hat{h}_{\mathbf{w},k} \left(\eta \right) \right)^{2}$$

where $\nabla_{\eta}\hat{h}_{\mathrm{w},k}\left(\eta\right) = 2\mathrm{Re}\left\{\mathbf{e}_{k}^{\mathrm{H}}\mathbf{\bar{w}}\right\}$ and $\nabla_{\eta}^{2}\hat{h}_{\mathrm{w},k}\left(\eta\right) =$ $-2\bar{\mathbf{w}}^{\mathrm{H}}\tilde{\mathbf{C}}_{\mathrm{w},k}\bar{\mathbf{w}}$, and $\bar{\mathbf{N}}_{\mathrm{w}}$ can be derived as

$$\bar{\mathbf{N}}_{\mathbf{w}} = -\sum_{k=1}^{K} \hat{g}_{\mathbf{w},k} \left(\boldsymbol{\eta} \right) \left(\begin{bmatrix} \tilde{\mathbf{C}}_{\mathbf{w},k} & \mathbf{0} \\ \mathbf{0} & \tilde{\mathbf{C}}_{\mathbf{w},k}^{\mathrm{T}} \end{bmatrix} + \zeta \begin{bmatrix} \mathbf{e}_{k} \\ \mathbf{e}_{k}^{*} \end{bmatrix} \begin{bmatrix} \mathbf{e}_{k} \\ \mathbf{e}_{k}^{*} \end{bmatrix}^{\mathrm{H}} \right)$$

$$+ \zeta \begin{bmatrix} \sum_{k=1}^{K} \hat{g}_{w,k} (\eta) \mathbf{e}_{k} \\ \sum_{k=1}^{K} \hat{g}_{w,k} (\eta) \mathbf{e}_{k}^{*} \end{bmatrix} \begin{bmatrix} \sum_{k=1}^{K} \hat{g}_{w,k} (\eta) \mathbf{e}_{k} \\ \sum_{k=1}^{K} \hat{g}_{w,k} (\eta) \mathbf{e}_{k}^{*} \end{bmatrix}^{H} . (96)$$

As a result, we have

$$\bar{\mathbf{N}}_{\mathbf{w}} \succeq \begin{bmatrix} \mathbf{M}_{\mathbf{w}} & \mathbf{0} \\ \mathbf{0} & \mathbf{M}_{\mathbf{w}}^{\mathrm{T}} \end{bmatrix}. \tag{97}$$

$$2\operatorname{Re}\left\{\sum_{k=1}^{K} h_{\mathbf{w},k}\left(\tilde{\mathbf{w}}^{(n)}\right) \left(\tilde{\boldsymbol{b}}_{\mathbf{w},k}^{\mathrm{H}} - \left(\tilde{\mathbf{w}}^{(n)}\right)^{\mathrm{H}} \tilde{\mathbf{C}}_{\mathbf{w},k}\right) \left(\tilde{\mathbf{w}}^{(m)} - \tilde{\mathbf{w}}^{(n)}\right)\right\},\tag{89}$$

$$\alpha = \lambda_{\min} \left(\tilde{\mathbf{N}}_{\mathbf{w}} \right) \overset{(a1)}{\geqslant} - \sum_{k=1}^{K} \tilde{g}_{\mathbf{w},k} \left(\eta \right) \left(\lambda_{\max} \left(\begin{bmatrix} \tilde{\mathbf{C}}_{\mathbf{w},k} & \mathbf{0} \\ \mathbf{0} & \tilde{\mathbf{C}}_{\mathbf{w},k}^{\mathrm{T}} \end{bmatrix} \right) + \zeta \lambda_{\max} \left(\begin{bmatrix} \mathbf{e}_{k} \\ \mathbf{e}_{k}^{*} \end{bmatrix} \begin{bmatrix} \mathbf{e}_{k} \\ \mathbf{e}_{k}^{*} \end{bmatrix}^{\mathrm{H}} \right) \right)$$

$$+ \zeta \lambda_{\min} \left(\begin{bmatrix} \sum_{k=1}^{K} \tilde{g}_{\mathbf{w},k} \left(\eta \right) \mathbf{e}_{k} \\ \sum_{k=1}^{K} \tilde{g}_{\mathbf{w},k} \left(\eta \right) \mathbf{e}_{k} \\ \sum_{k=1}^{K} \tilde{g}_{\mathbf{w},k} \left(\eta \right) \mathbf{e}_{k}^{*} \end{bmatrix} \begin{bmatrix} \sum_{k=1}^{K} \tilde{g}_{\mathbf{w},k} \left(\eta \right) \mathbf{e}_{k} \\ \sum_{k=1}^{K} \tilde{g}_{\mathbf{w},k} \left(\eta \right) \mathbf{e}_{k}^{*} \end{bmatrix}^{\mathrm{H}} \right)$$

$$\overset{(a2)}{=} - \sum_{k=1}^{K} \tilde{g}_{\mathbf{w},k} \left(\eta \right) \left(\lambda_{\max} \left(\tilde{\mathbf{C}}_{\mathbf{w},k} \right) + 2\zeta \mathbf{e}_{k}^{\mathrm{H}} \mathbf{e}_{k} \right) \overset{(a3)}{\geqslant} - \max_{k} \left\{ \lambda_{\max} \left(\tilde{\mathbf{C}}_{\mathbf{w},k} \right) \right\} - 2\zeta \max_{k} \left\{ \|\mathbf{e}_{k}\|_{2}^{2} \right\}.$$

$$(100)$$

$$\|\mathbf{e}_{k}\|_{2}^{2} = \|\tilde{\boldsymbol{b}}_{w,k} - \tilde{\mathbf{C}}_{w,k}^{H} (\tilde{\mathbf{w}}^{n} + \eta (\tilde{\mathbf{w}}^{m} - \tilde{\mathbf{w}}^{n}))\|_{2}^{2}$$

$$= \|\tilde{\boldsymbol{b}}_{w,k}\|_{2}^{2} + \|\tilde{\mathbf{C}}_{w,k}^{H} (\tilde{\mathbf{w}}^{n} + \eta (\tilde{\mathbf{w}}^{m} - \tilde{\mathbf{w}}^{n}))\|_{2}^{2} - 2\operatorname{Re} \left\{ \tilde{\boldsymbol{b}}_{w,k}^{H} \tilde{\mathbf{C}}_{w,k}^{H} (\tilde{\mathbf{w}}^{n} + \eta (\tilde{\mathbf{w}}^{m} - \tilde{\mathbf{w}}^{n})) \right\}$$

$$\stackrel{(a4)}{\leq} \lambda_{\max} \left(\tilde{\mathbf{C}}_{w,k} \tilde{\mathbf{C}}_{w,k}^{H} \right) \|\tilde{\mathbf{w}}^{n} + \eta (\tilde{\mathbf{w}}^{m} - \tilde{\mathbf{w}}^{n})\|_{2}^{2} + \|\tilde{\boldsymbol{b}}_{w,k}\|_{2}^{2} - 2\operatorname{Re} \left\{ \tilde{\boldsymbol{b}}_{w,k}^{H} \tilde{\mathbf{C}}_{w,k}^{H} (\tilde{\mathbf{w}}^{n} + \eta (\tilde{\mathbf{w}}^{m} - \tilde{\mathbf{w}}^{n})) \right\}$$

$$\stackrel{(a5)}{\leq} P \lambda_{\max} \left(\tilde{\mathbf{C}}_{w,k} \tilde{\mathbf{C}}_{w,k}^{H} \right) + \|\tilde{\boldsymbol{b}}_{w,k}\|_{2}^{2} + 2\sqrt{P} \|\tilde{\mathbf{C}}_{w,k} \tilde{\boldsymbol{b}}_{w,k}\|_{2}^{2}.$$

$$(101)$$

Choosing $\mathbf{M}_{\mathrm{w}} = \bar{\alpha} \mathbf{I} = \lambda_{\min} \left(\bar{\mathbf{N}}_{\mathrm{w}} \right) \mathbf{I}$, (88) can be rewritten as $\bar{f} \left(\tilde{\mathbf{w}} | \tilde{\mathbf{w}}^{(n)} \right) = \bar{c}_{\mathrm{w}} + 2 \operatorname{Re} \left\{ \bar{\mathbf{v}}_{\mathrm{w}}^{\mathrm{H}} \tilde{\mathbf{w}} \right\} + \alpha \tilde{\mathbf{w}}^{\mathrm{H}} \tilde{\mathbf{w}}$, (98)

where $\bar{\mathbf{v}}_{\mathrm{w}}$ and \bar{c}_{w} are given in (72a) and (72b), respectively. However, the complexity of computing α cannot be ignored. We introduce the following lemmas to reduce the complexity:

(a1)

- 1) $\lambda_{\min}(\mathbf{A}) + \lambda_{\min}(\mathbf{B}) \leq \lambda_{\min}(\mathbf{A} + \mathbf{B})$, if **A** and **B** are Hermitian matrices [54]:
- 2) $\lambda_{\max}(\mathbf{A}) = \operatorname{Tr}(\mathbf{A})$ and $\lambda_{\min}(\mathbf{A}) = 0$, if **A** is a rank one matrix [54];
- 3) $\sum_{m=1}^{(m)} a_m b_m \leqslant \max_{m=1}^{(m)} \{b_m\}$, if $a_m, b_m \geqslant 0$ and $\sum_{m=1}^{(m)} a_m = 1$ [55, Theorem 30];
- 4) $\operatorname{Tr}(\mathbf{AB}) \leq \lambda_{\max}(\mathbf{A}) \operatorname{Tr}(\mathbf{B})$, if **A** and **B** are positive semidefinite matrices [54].

Additionally, it can be readily verified that (a5)

1) $-\sqrt{P}\|\mathbf{B}\mathbf{c}\|_2$ is the solution to the following problem: $\min_{\mathbf{x}} \operatorname{Re} \left\{ \mathbf{c}^{\mathrm{H}} \mathbf{B}^{\mathrm{H}} \mathbf{x} \right\} \tag{99a}$

s.t.
$$\mathbf{x}^{\mathrm{H}}\mathbf{x} \leqslant P$$
. (99b)

Using the inequalities (a1) and (a3) and the equality (a2), a lower bound for α can be derived as given in (100), shown at the top of the page.

Since $\tilde{\mathbf{w}} = \tilde{\mathbf{w}}^{(n)} + \eta \left(\tilde{\mathbf{w}}^{(m)} - \tilde{\mathbf{w}}^{(n)} \right), \ \eta \in [0, 1],$ we obtain $\|\tilde{\mathbf{w}} = \tilde{\mathbf{w}}^{(n)} + \eta \left(\tilde{\mathbf{w}}^{(m)} - \tilde{\mathbf{w}}^{(n)} \right) \|_2 \le \sqrt{P}$. Furthermore, using (a4) and (a5), an upper bound for $\|\mathbf{e}_k\|_2^2$ is given in (101), shown at the top of the page.

Finally, by combining (100) with (101), we obtain the simple lower bound $\bar{\alpha}$ for α in (72c).

Hence, the proof is completed.

REFERENCES

- IMT Vision Framework and Overall Objectives of the Future Development Of IMT for 2020 and Beyond, document ITU Recommendation M. 2083, ITU-R, Sep. 2015.
- [2] F. Tariq, M. R. A. Khandaker, K.-K. Wong, M. A. Imran, M. Bennis, and M. Debbah, "A speculative study on 6G," *IEEE Wireless Commun.*, vol. 27, no. 4, pp. 118–125, Aug. 2020.
- [3] C. Pan et al., "Reconfigurable intelligent surfaces for 6G systems: Principles, applications, and research directions," *IEEE Commun. Mag.*, vol. 59, no. 6, pp. 14–20, Jun. 2021.

- [4] W. Chen, X. Ma, Z. Li, and N. Kuang, "Sum-rate maximization for intelligent reflecting surface based terahertz communication systems," in *Proc. IEEE/CIC Int. Conf. Commun. Workshops China (ICCC Work-shops)*, Aug. 2019, pp. 153–157.
- [5] C. Liaskos, S. Nie, A. Tsioliaridou, A. Pitsillides, S. Ioannidis, and I. Akyildiz, "A new wireless communication paradigm through software-controlled metasurfaces," *IEEE Commun. Mag.*, vol. 56, no. 9, pp. 162–169, Sep. 2018.
- [6] Z. Peng, Z. Zhang, C. Pan, L. Li, and A. L. Swindlehurst, "Multiuser full-duplex two-way communications via intelligent reflecting surface," *IEEE Trans. Signal Process.*, vol. 69, pp. 837–851, 2021.
- [7] Q. Wu, S. Zhang, B. Zheng, C. You, and R. Zhang, "Intelligent reflecting surface-aided wireless communications: A tutorial," *IEEE Trans. Commun.*, vol. 69, no. 5, pp. 3313–3351, May 2021.
- [8] M. Di Renzo et al., "Smart radio environments empowered by reconfigurable intelligent surfaces: How it works, state of research, and the road ahead," *IEEE J. Sel. Areas Commun.*, vol. 38, no. 11, pp. 2450–2525, Nov. 2020.
- [9] B. Zheng et al., "Intelligent reflecting surface assisted multi-user OFDMA: Channel estimation and training design," *IEEE Trans. Wireless Commun.*, vol. 19, no. 12, pp. 8315–8329, Dec. 2020.
- [10] M. D. Renzo et al., "Reconfigurable intelligent surfaces vs. relaying: Differences, similarities, and performance comparison," *IEEE Open J. Commun. Soc.*, vol. 1, pp. 798–807, 2020.
- [11] M. D. Renzo, F. H. Danufane, and S. Tretyakov, "Communication models for reconfigurable intelligent surfaces: From surface electromagnetics to wireless networks optimization," *Proc. IEEE*, vol. 110, no. 9, pp. 1164–1209, Sep. 2022.
- [12] Q. Wu and R. Zhang, "Intelligent reflecting surface enhanced wireless network via joint active and passive beamforming," *IEEE Trans. Wireless Commun.*, vol. 18, no. 11, pp. 5394–5409, Nov. 2019.
- [13] Q. Wu and R. Zhang, "Towards smart and reconfigurable environment: Intelligent reflecting surface aided wireless network," *IEEE Commun. Mag.*, vol. 58, no. 1, pp. 106–112, Jan. 2020.
- [14] X. Yu, D. Xu, and R. Schober, "Enabling secure wireless communications via intelligent reflecting surfaces," in *Proc. IEEE Global Commu. Conf. (GLOBECOM)*, Waikoloa, HI, USA, Dec. 2019, pp. 1–6.
- [15] J. Liu, J. Zhang, Q. Zhang, J. Wang, and X. Sun, "Secrecy rate analysis for reconfigurable intelligent surface-assisted MIMO communications with statistical CSI," *China Commun.*, vol. 18, no. 3, pp. 52–62, Mar. 2021.
- [16] D. Xu, X. Yu, Y. Sun, D. W. K. Ng, and R. Schober, "Resource allocation for secure IRS-assisted multiuser MISO systems," in *Proc. IEEE Globecom Workshops (GC Wkshps)*, Dec. 2019, pp. 1–6.
- [17] K. Cumanan, Z. Ding, B. Sharif, G. Y. Tian, and K. K. Leung, "Secrecy rate optimizations for a MIMO secrecy channel with a multiple-antenna eavesdropper," *IEEE Trans. Veh. Technol.*, vol. 63, no. 4, pp. 1678–1690, May 2014.
- [18] A. Almohamad et al., "Smart and secure wireless communications via reflecting intelligent surfaces: A short survey," *IEEE Open J. Commun.* Soc., vol. 1, pp. 1442–1456, 2020.

- [19] M. Cui, G. Zhang, and R. Zhang, "Secure wireless communication via intelligent reflecting surface," *IEEE Wireless Commun. Lett.*, vol. 8, no. 5, pp. 1410–1414, Oct. 2019.
- [20] L. Yang, J. Yang, W. Xie, M. O. Hasna, T. Tsiftsis, and M. D. Renzo, "Secrecy performance analysis of RIS-aided wireless communication systems," *IEEE Trans. Veh. Technol.*, vol. 69, no. 10, pp. 12296–12300, Oct. 2020.
- [21] X. Yu, D. Xu, Y. Sun, D. W. K. Ng, and R. Schober, "Robust and secure wireless communications via intelligent reflecting surfaces," *IEEE J. Sel. Areas Commun.*, vol. 38, no. 11, pp. 2637–2652, Nov. 2020.
- [22] H. Yang, Z. Xiong, J. Zhao, D. Niyato, L. Xiao, and Q. Wu, "Deep reinforcement learning-based intelligent reflecting surface for secure wireless communications," *IEEE Trans. Wireless Commun.*, vol. 20, no. 1, pp. 375–388, Jan. 2021.
- [23] G. Sun, X. Tao, N. Li, and J. Xu, "Intelligent reflecting surface and UAV assisted secrecy communication in millimeter-wave networks," *IEEE Trans. Veh. Technol.*, vol. 70, no. 11, pp. 11949–11961, Nov. 2021.
- [24] E. Björnson, J. Hoydis, M. Kountouris, and M. Debbah, "Massive MIMO systems with non-ideal hardware: Energy efficiency, estimation, and capacity limits," *IEEE Trans. Inf. Theory*, vol. 60, no. 11, pp. 7112–7139, Nov. 2014.
- [25] H. Shen, W. Xu, S. Gong, C. Zhao, and D. W. K. Ng, "Beamforming optimization for IRS-aided communications with transceiver hardware impairments," *IEEE Trans. Commun.*, vol. 69, no. 2, pp. 1214–1227, Feb. 2021.
- [26] G. Zhou, C. Pan, H. Ren, K. Wang, and Z. Peng, "Secure wireless communication in RIS-aided MISO system with hardware impairments," *IEEE Wireless Commun. Lett.*, vol. 10, no. 6, pp. 1309–1313, Jun. 2021.
- [27] Q. Chen, M. Li, X. Yang, R. Alturki, M. D. Alshehri, and F. Khan, "Impact of residual hardware impairment on the IoT secrecy performance of RIS-assisted NOMA networks," *IEEE Access*, vol. 9, pp. 42583–42592, 2021.
- [28] Z. Xing, R. Wang, J. Wu, and E. Liu, "Achievable rate analysis and phase shift optimization on intelligent reflecting surface with hardware impairments," *IEEE Trans. Wireless Commun.*, vol. 20, no. 9, pp. 5514–5530, Sep. 2021.
- [29] S. Abeywickrama, R. Zhang, Q. Wu, and C. Yuen, "Intelligent reflecting surface: Practical phase shift model and beamforming optimization," *IEEE Trans. Commun.*, vol. 68, no. 9, pp. 5849–5863, Sep. 2020.
- [30] H. Li, W. Cai, Y. Liu, M. Li, Q. Liu, and Q. Wu, "Intelligent reflecting surface enhanced wideband MIMO-OFDM communications: From practical model to reflection optimization," *IEEE Trans. Commun.*, vol. 69, no. 7, pp. 4807–4820, Jul. 2021.
- [31] W. Cai, H. Li, M. Li, and Q. Liu, "Practical modeling and beamforming for intelligent reflecting surface aided wideband systems," *IEEE Commun. Lett.*, vol. 24, no. 7, pp. 1568–1571, Jul. 2020.
- [32] J. Zhu, D. W. K. Ng, N. Wang, R. Schober, and V. K. Bhargava, "Analysis and design of secure massive MIMO systems in the presence of hardware impairments," *IEEE Trans. Wireless Commun.*, vol. 16, no. 3, pp. 2001–2016, Jan. 2017.
- [33] Y. Liu, E. Liu, and R. Wang, "Energy efficiency analysis of intelligent reflecting surface system with hardware impairments," in *Proc. GLOBE-COM IEEE Global Commun. Conf.*, Dec. 2020, pp. 1–6.
- [34] J. Zhu, R. Schober, and V. K. Bhargava, "Secure transmission in multicell massive MIMO systems," *IEEE Trans. Wireless Commun.*, vol. 13, no. 9, pp. 4766–4781, Sep. 2014.
- [35] Y. Wu, A. Khisti, C. Xiao, G. Caire, K.-K. Wong, and X. Gao, "A survey of physical layer security techniques for 5G wireless networks and challenges ahead," *IEEE J. Sel. Areas Commun.*, vol. 36, no. 4, pp. 679–695, Apr. 2018.
- [36] Z. Wang, L. Liu, and S. Cui, "Channel estimation for intelligent reflecting surface assisted multiuser communications: Framework, algorithms, and analysis," *IEEE Trans. Wireless Commun.*, vol. 19, no. 10, pp. 6607–6620, Jun. 2020.
- [37] X. Guan, Q. Wu, and R. Zhang, "Anchor-assisted channel estimation for intelligent reflecting surface aided multiuser communication," *IEEE Trans. Wireless Commun.*, vol. 21, no. 6, pp. 3764–3778, Jun. 2022.
- [38] H. Ren, X. Liu, C. Pan, Z. Peng, and J. Wang, "Performance analysis for RIS-aided secure massive MIMO systems with statistical CSI," *IEEE Wireless Commun. Lett.*, vol. 12, no. 1, pp. 124–128, Jan. 2023.
- [39] Q. Zhang, S. Jin, K.-K. Wong, H. Zhu, and M. Matthaiou, "Power scaling of uplink massive MIMO systems with arbitrary-rank channel means," *IEEE J. Sel. Topics Signal Process.*, vol. 8, no. 5, pp. 966–981, Oct. 2014.

- [40] K. Shen and W. Yu, "Fractional programming for communication systems—Part I: Power control and beamforming," *IEEE Trans. Signal Process.*, vol. 66, no. 10, pp. 2616–2630, May 2018.
- [41] X. Guan, Q. Wu, and R. Zhang, "Intelligent reflecting surface assisted secrecy communication: Is artificial noise helpful or not?" *IEEE Wireless Commun. Lett.*, vol. 9, no. 6, pp. 778–782, Jun. 2020.
- [42] G. Zhou, C. Pan, H. Ren, K. Wang, K. K. Chai, and K.-K. Wong, "User cooperation for IRS-aided secure SWIPT MIMO systems," 2020, arXiv:2006.05347.
- [43] Z. Peng, R. Weng, C. Pan, G. Zhou, M. D. Renzo, and A. L. Swindlehurst, "Robust transmission design for RIS-assisted secure multiuser communication systems in the presence of hardware impairments," 2022, arXiv:2202.11860.
- [44] X. Zhang, Matrix Analysis and Applications. Beijing, China: Tsinghua Univ. Press, 2004.
- [45] M. A. Vázquez, L. Blanco, and A. I. Pérez-Neira, "Spectrum sharing backhaul satellite-terrestrial systems via analog beamforming," *IEEE J. Sel. Topics Signal Process.*, vol. 12, no. 2, pp. 270–281, May 2018.
- [46] G. Zhou, C. Pan, H. Ren, K. Wang, M. Di Renzo, and A. Nallanathan, "Robust beamforming design for intelligent reflecting surface aided MISO communication systems," *IEEE Wireless Commun. Lett.*, vol. 9, no. 10, pp. 1658–1662, Oct. 2020.
- [47] A. Ben-Tal and A. Nemirovski, Lectures on Modern Convex Optimization: Analysis, Algorithms, and Engineering Applications. Philadelphia, PA, USA: Society for Industrial and Applied Mathematics, 2001.
- [48] S. Xu, "Smoothing method for minimax problems," Comput. Optim. Appl., vol. 20, no. 3, pp. 267–279, 2001.
- [49] G. Zhou, C. Pan, H. Ren, K. Wang, and A. Nallanathan, "Intelligent reflecting surface aided multigroup multicast miso communication systems," *IEEE Trans. Signal Process.*, vol. 68, pp. 3236–3251, 2020.
- [50] Y. Sun, P. Babu, and D. P. Palomar, "Majorization-minimization algorithms in signal processing, communications, and machine learning," *IEEE Trans. Signal Process.*, vol. 65, no. 3, pp. 794–816, Feb. 2017.
- [51] R. Varadhan and C. Roland, "Simple and globally convergent methods for accelerating the convergence of any EM algorithm," *Scand. J. Statist. Theory Appl.*, vol. 35, no. 2, pp. 335–353, 2008.
- [52] The MOSEK Optimization Toolbox for MATLAB Manual, Version 9.2 (Revision 14), MOSEK-ApS, Copenhagen, Denmark, Jun. 2020.
- [53] Q. Q. Wu and R. Zhang, "Beamforming optimization for wireless network aided by intelligent reflecting surface with discrete phase shifts," *IEEE Trans. Commun.*, vol. 68, no. 3, pp. 1838–1851, May 2020.
- [54] H. Lütkepohl, Handbook Matrices. New York, NY, USA: Wiley, 1996.
- [55] J. R. Magnus and H. Neudecker, Matrix Differential Calculus With Applications in Statistics and Econometrics. Hoboken, NJ, USA: Wiley, 1988.



Zhangjie Peng received the B.S. degree in communication and information engineering from Southwest Jiaotong University, Chengdu, China, in 2004, and the M.S. and Ph.D. degrees in communication and information engineering from Southeast University, Nanjing, China, in 2007 and 2016, respectively.

He is currently an Associate Professor with the College of Information, Mechanical and Electrical Engineering, Shanghai Normal University, Shanghai, China. His research interests include reconfigurable intelligent surface (RIS), cooperative communica-

tions, information theory, physical layer security, and machine learning for wireless communications.



Ruisong Weng received the B.E. degree from the Software Institute, Nanjing University, Nanjing, China, in 2020. He is currently pursuing the M.E. degree with the College of Information, Mechanical and Electrical Engineering, Shanghai Normal University, Shanghai, China.

His major research interests include reconfigurable intelligent surface (RIS), physical layer security, mobile edge computing, and signal processing.



Cunhua Pan (Senior Member, IEEE) received the B.S. and Ph.D. degrees from the School of Information Science and Engineering, Southeast University, Nanjing, China, in 2010 and 2015, respectively.

From 2015 to 2016, he was a Research Associate at the University of Kent, U.K. He held a post-doctoral position at the Queen Mary University of London, U.K., from 2016 and 2019, where he was a Lecturer, from 2019 to 2021. Since 2021, he has been a Full Professor with Southeast University. He has published more than 120 IEEE journal arti-

cles. His research interests mainly include reconfigurable intelligent surfaces (RIS), intelligent reflection surface (IRS), ultra-reliable low latency communication (URLLC), machine learning, UAV, the Internet of Things, and mobile edge computing. He serves as a TPC Member for numerous conferences, such as IEEE ICC and IEEE GLOBECOM. He received the IEEE ComSoc Leonard G. Abraham Prize in 2022 and the IEEE ComSoc Asia-Pacific Outstanding Young Researcher Award in 2022. He is the Workshop Organizer in IEEE ICCC 2021 on the topic of Reconfigurable Intelligent Surfaces for Next Generation Wireless Communications (RIS for 6G Networks) and IEEE GLOBECOM 2021 on the topic of Reconfigurable Intelligent Surfaces for future wireless communications. He is currently the Workshops Officer and the Symposia Officer for Reconfigurable Intelligent Surfaces Emerging Technology Initiative. He serves as the Student Travel Grant Chair for ICC 2019. He is the Workshop Chair for IEEE WCNC 2024 and the TPC Co-Chair of IEEE ICCT 2022. He is currently an Editor of IEEE WIRELESS COM-MUNICATIONS LETTERS, IEEE COMMUNICATIONS LETTERS, and IEEE ACCESS. He serves as a Guest Editor for IEEE JOURNAL OF SELECTED TOPICS IN SIGNAL PROCESSING on the Special Issue on xURLLC in 6G: Next Generation Ultra-Reliable and Low-Latency Communications. He also serves as a Leading Guest Editor for IEEE JOURNAL OF SELECTED TOPICS IN SIGNAL PROCESSING Special Issue on Advanced Signal Processing for Reconfigurable Intelligent Surface-Aided 6G Networks, IEEE Vehicular Technology Magazine on the Special Issue on Backscatter and Reconfigurable Intelligent Surface Empowered Wireless Communications in 6G, IEEE OPEN JOURNAL OF VEHICULAR TECHNOLOGY on the Special Issue of Reconfigurable Intelligent Surface Empowered Wireless Communications in 6G and Beyond, and IEEE ACCESS Special Issue on Reconfigurable Intelligent Surface Aided Communications for 6G and Beyond.



Gui Zhou (Member, IEEE) received the B.S. and M.E. degrees from the School of Information and Electronics, Beijing Institute of Technology, Beijing, China, in 2015 and 2019, respectively, and the Ph.D. degree from the School of Electronic Engineering and Computer Science, Queen Mary University of London, U.K., in 2022.

She is currently a Humboldt Post-Doctoral Research Fellow with the Institute for Digital Communications, Friedrich-Alexander-Universität Erlangen-Nürnberg (FAU), Erlangen, Germany. Her

major research interests include reconfigurable intelligent surfaces (RIS) and array signal processing.



Marco Di Renzo (Fellow, IEEE) received the Laurea (cum laude) and Ph.D. degrees in electrical engineering from the University of L'Aquila, Italy, in 2003 and 2007, respectively, and the Habilitation à Diriger des Recherches (Doctor of Science) degree from University Paris-Sud (now Paris-Saclay University), France, in 2013. He is currently a CNRS Research Director (Professor) and the Head of the Intelligent Physical Communications Group with the Laboratory of Signals and Systems (L2S), CNRS, CentraleSupelec, Paris-Saclay Uni-

versity, Paris, France. In Paris-Saclay University, he serves as the Coordinator for the Communications and Networks Research Area of the Laboratory of Excellence DigiCosme. Also, he is a member of the Admission and Evaluation Committee of the Ph.D. School on Information and Communication Technologies, and a member of the Evaluation Committee of the Graduate School in Computer Science, Paris-Saclay University. He is a Founding Member and the Academic Vice Chair of the Industry Specification Group (ISG) on Reconfigurable Intelligent Surfaces (RIS) within the European Telecommunications Standards Institute (ETSI), where he serves as the Rapporteur for the work item on communication models, channel models, and evaluation methodologies. He is a fellow of the IET, AAIA, and Vebleo; an Ordinary Member of the European Academy of Sciences and Arts and the Academia Europaea; and a Highly Cited Researcher. He is also a Fulbright Fellow with the City University of New York, USA. He was a Nokia Foundation Visiting Professor and a Royal Academy of Engineering Distinguished Visiting Fellow. His recent research awards include the 2021 EURASIP Best Paper Award, the 2022 IEEE COMSOC Outstanding Paper Award, and the 2022 Michel Monpetit Prize conferred by the French Academy of Sciences. He serves as the Editor-in-Chief of IEEE COMMUNICATIONS LETTERS.



A. Lee Swindlehurst (Fellow, IEEE) received the B.S. and M.S. degrees in electrical engineering from Brigham Young University (BYU) in 1985 and 1986, respectively, and the Ph.D. degree in electrical engineering from Stanford University in 1991. He was with the Department of Electrical and Computer Engineering, BYU, from 1990 to 2007, where he served as the Department Chair from 2003 to 2006. From 1996 to 1997, he held a joint appointment as a Visiting Scholar at Uppsala University and the Royal Institute of Technology, Sweden.

From 2006 to 2007, he was on leave working as a Vice President of Research for ArrayComm LLC, San Jose, CA, USA. Since 2007, he has been a Professor with the Electrical Engineering and Computer Science Department, University of California Irvine, where he served as an Associate Dean for Research and Graduate Studies in the Samueli School of Engineering from 2013 to 2016. From 2014 to 2017, he was a Hans Fischer Senior Fellow with the Institute for Advanced Studies, Technical University of Munich. In 2016, he was elected as a Foreign Member of the Royal Swedish Academy of Engineering Sciences (IVA). His research focuses on array signal processing for radar, wireless communications, and biomedical applications. He has over 300 publications in these areas. He received the 2022 IEEE Signal Processing Society's Claude Shannon-Harry Nyquist Technical Achievement Award. He has also received numerous article awards including the 2000 IEEE W. R. G. Baker Prize Paper Award, the 2006 IEEE Communications Society Stephen O. Rice Prize in communication theory, the 2006, 2010, and 2022 IEEE Signal Processing Society's Best Paper Awards, the 2017 IEEE Signal Processing Society Donald G. Fink Overview Paper Award, and the Best Paper Award at the 2020 IEEE International Conference on Communications. He was the inaugural Editor-in-Chief of the IEEE JOURNAL OF SELECTED TOPICS IN SIGNAL PROCESSING.